# Texas College of Osteopathic Medicine

First Annual

# RESEARCH APPRECIATION PROGRAM (RAP)

## MARCH 22, 1993

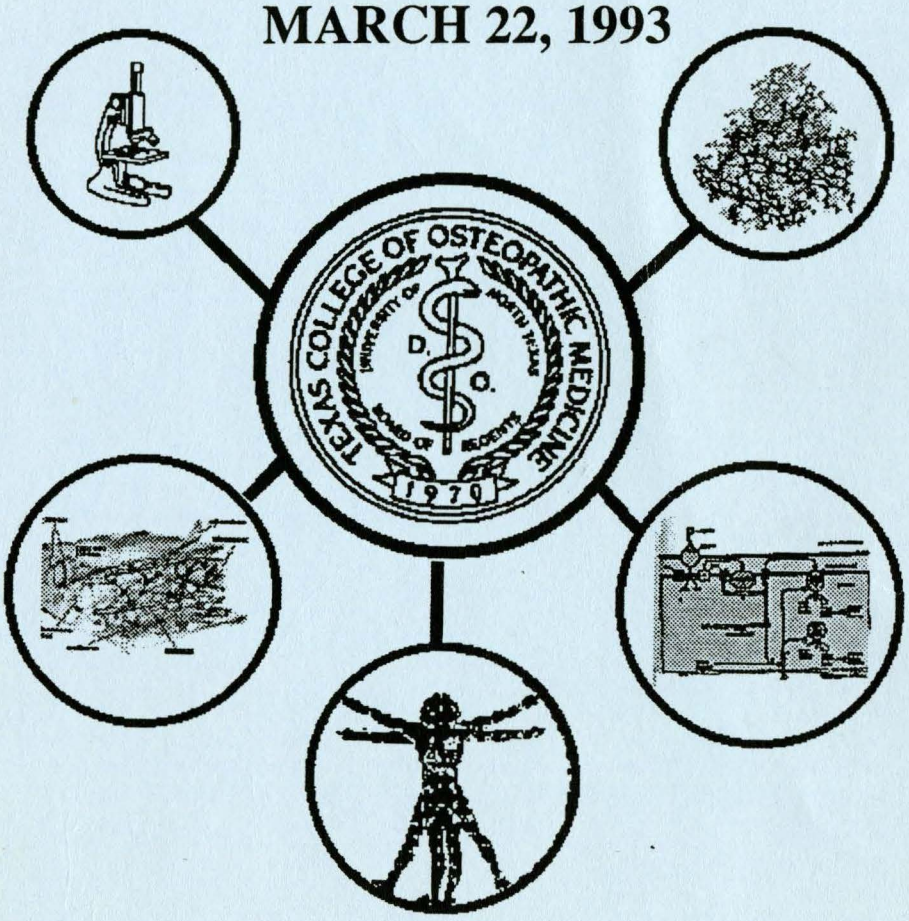


Sponsored by

OFFICE OF GRADUATE STUDIES
OFFICE OF RESEARCH
GRADUATE STUDENT ASSOCIATION
STUDENT GOVERNMENT ASSOCIATION

Texas College of Osteopathic Medicine

Research Appreciation Program (RAP)

March 22, 1993

# Table of Contents

# First Author Index

* Graduate Student
** Medical Student
*** Fellow or Intern

| Last Name | Abstract Number |
|---|---|
| Leu *** | 27 |
| Li * | 94 |
| Liu * | 12, 37 |
| Longlet * | 43 |
| Lurie | 70 |
| Mallet | 47 |
| Mallick *** | 1 |
| Manor *** | 59 |
| Mateo * | 57 |
| Matsumoto | 84 |
| McClure * | 28 |
| Mendoza-Alvarez *** | 31 |
| Mia | 63 |
| Nalabolu * | 29 |
| Napier * | 58 |
| Nelson | 5 |
| Pacheco-Rodriguez * | 30, 33 |
| Page *** | 69 |
| Papa | 71 |
| Paranjape * | 7 |
| Parker * | 46 |
| Peltier * | 95 |
| Pertusi | 68 |
| Postlethwait * | 36 |
| Quist | 44 |
| Rao *** | 21, 22, 25 |
| Reese | 76 |
| Reeves * | 79 |
| Rege * | 26 |
| Rezazadeh *** | 97 |
| Roque | 85 |
| Rubin | 74 |
| Schofield ** | 61 |
| Sheedlo | 87 |
| Shi | 39, 40 |
| Stutts * | 96, 99 |
| Sun *** | 19, 20 |
| Sundarrajan * | 8 |

| Last Name | Abstract Number |
|---|---|
| Tai* | 24 |
| Talent | 3 |
| Taylor, C. M. * | 2 |
| Taylor, M. *** | 66, 67 |
| Taylor, S. * | 60 |
| Tripathy *** | 15 |
| Vanderheiden *** | 72 |
| Verstappen * | 83 |
| Wallis *** | 98 |
| Walters * | 11 |
| Wang * | 48 |
| Wenham * | 10 |
| Williams *** | 52 |
| Williamson * | 42 |
| Wordinger | 13 |
| Wright | 38 |
| Xu * | 100 |
| Yuksel | 17, 18 |
| Zhou * | 82 |

41 GS
5 MS
23 Fellows/Interns

# Aging

# Abstracts 1 - 5

HETEROGENEITY OF BRAIN-REACTIVE AUTOANTIBODIES IN AGING C57BL/6 MICE. S. Mallick, R. L. Luedtke, M. J. Forster and H. Lal. Texas Coll. of Osteopathic Med., Ft. Worth, TX 76107.

Previous studies have implicated an age-dependent increase in the expression of autoimmune brain-reactive antibodies in mammals. Sera, at 1:500 dilution, from old (20-24 mo), middle-aged (10-12 mo), and young (2-4 mo) male C57BL/6 mice were compared using an immunoblot assay with a peroxidase-conjugated detection system. Cytosolic proteins prepared from the brains of young C57BL/6 mice were used as antigens. Four immunoreactive banding patterns were observed: A) a single predominant band; B) more than one predominant band; C) a generalized banding pattern; and NR) no reactivity. Of the 15 young mice tested, 13% were positive for bands below 45 kDa. In contrast, 30% of the middle-aged mice and 60% of the old mice tested showed an autoimmune response. Of the old positive mice, 72%, 11%, and 17% were categorized in the above subgroups A, B, and C, respectively. A 170 kDa antigen was identified in 50% of the Group A mice while the remainder of the mice in the same group identified antigens between 40-55 kDa. In order to assess the tissue specificity of the autoantibody response, cytosolic proteins from spleen thymus, heart, lung, and liver were screened. The autoantibodies bound antigens in each of the tissues that were examined. However, initial results suggest that the 170 kDa antigen is expressed only in brain tissue. Summarizing, a greater incidence of autoreactive antibodies has been observed in aged animals. While variability between animals was observed, individual autoimmune responses appear to be restricted.

Supported by NIH grants AG06182 (MJF) and AG07695 (HL).

DIETARY RESTRICTION DELAYS AGE-RELATED DECLINES IN RECENT MEMORY CAPACITY OF AGING B6D2F$_1$/NNia MICE. C.M.Taylor, H.Lal, M.J.Forster, Department of Pharmacology, Texas College of Osteopathic Medicine, Fort Worth, TX 76107.

Longitudinal studies were conducted to determine if the neural changes responsible for cognitive decline would be decelerated by long-term dietary restriction, a procedure which results in increased longevity in rodents. Male B6D2F$_1$ mice fed ad libitum or reared under dietary restriction (60% of ad libitum begining at 4 months) were tested for recent memory capacity using a delayed reversal task (Forster & Lal, Biomed. Environ. Sci.,4,144,1991) at 10 and 22 months of age. This task involved training of a reversal set which serves as a baseline for memory performance testing across the lifespan. All mice learned the reversal set to equivalent performance levels at both ages. The ad-libitum fed mice showed significant age related decline in recent memory capacity, as evidenced by an increased rate of memory decay following the information acquisition. There was no change in memory performance of diet restricted mice as a function of age, although restriction conferred a slight performance disadvantage relative to ad libitum fed mice at 10 months of age. Subsequent analyses indicated that the latter effect was independent of age and could be attributed to short-term consequences of diet restriction. Overall, the results suggest that dietary restriction may acutely influence the level of cognitive performance, as well as retard age-associated changes responsible for cognitive decline. Supported by NIA grants AG07695 (H.L.) and AG06182 (M.F.).

**AGING OF HUMAN SKIN: IDENTIFICATION OF AGING-RELATED CHANGES BY USE OF TWO-DIMENSIONAL GEL ELECTROPHORESIS.** J.M. Talent, S.D. Dimitrejevich, K.Ü. Yüksel, and R.W. Gracy, The Molecular Aging Unit and the Wound Healing Unit, Dept. of Biochemistry and Molecular Biology, Texas College of Osteopathic Medicine/ University of North Texas, Fort Worth, TX 76107

It is not known whether the specific modifications induced by the two aging processes (chronological aging *vs.* photo-aging) are identical. We have initiated studies to quantify the modifications to proteins in skin, both *in vivo* and *in vitro,* during normal aging and/or as a consequence of chronic sun exposure. Two-dimensional mapping by gel electrophoresis (2-D PAGE) is being utilized as a screening mechanism. The initial objectives of this project have been 1) optimization of conditions for resolution of the proteins of human skin, 2) optimization of methods for cell harvesting and solubilization, 3) verification of reproducibility of the two above procedures, 4) preliminary examination of changes in proteins in the skin with age. Age related differences were observed in the 2-D PAGE profiles of both epidermis and fibroblasts. *In vivo* studies continue on the effects of photoaging/ chronological aging in human skin. (Supported by Johnson & Johnson Consumer Products Inc. and the Texas Advanced Technology and Research Program (#2147) ).

# EFFECT OF HYPERBARIC OXYGEN ON NORMAL HUMAN SKIN CELLS AND THE SKIN TISSUE EQUIVALENTS.

L. COOPER[1], S. D. DIMITRIJEVICH[1], A. SMITH[2], J. WILLSON[3], S. BUCHANON[2] AND R.W. GRACY[1]. DEPARTMENT OF BIOCHEMISTRY AND MOLECULAR BIOL.[1], DEPT. OF SURGERY[2], CLINICAL HYPERBARIC MEDICINE GROUP[3].

A critical stage in wound healing in skin is the development and maturation of the epidermis. In the aged, as well as in some pathologies (e.g. diabetes), this repair process is compromised. The human Skin Equivalent (SE), is an excellent tool for studying the effect of aging on skin wound healing, since it excludes the systemic complications encountered *in vivo.*

The goal of this project is to examine the effect of hyperbaric oxygen on the epidermopoiesis of the SE constructed using infant skin cells, and compare this with the hyperoxic effect on the SE composed of cells from aged donors. The effect on the basal keratinocyte proliferation and motility and epidermal differentiation and maturation will be evaluated. The results from these studies will not only answer some questions about cutaneous wound healing, but will also provide insight into the process of autonomous oxygen utilization in peripheral human tissue.

Supported by a Pilot Grant from the North Texas Institute for Education and Research in Aging.

# LEVELS OF TRIOSE PHOSPHATE ISOMERASE EXPRESSION IN DERMAL FIBROBLASTS OF VARYING AGE

John P. Nelson, Jr., S. Dan Dimitrijevich and Robert W. Gracy, Dept. of Biochem and Mol. Biol., TCOM/UNT, Ft. Worth, TX.

Levels of expression of the triose phosphate isomerase (TPI) gene were examined in cells of various aged donors. Dermal fibroblasts were cultured in vitro and total RNA extracted from confluent, early passage cells. RNA analysis was accomplished by both Northern and slot hybridization using a plasmid containing the entire coding and 3' untranslated regions of TPI as the probe's template via the random primer labeling system. Preliminary results indicate that the level of TPI message in these cells is extremely low requiring the use of poly $(A)^+$ mRNA in order to get sufficient signal.

Supported by Grants from NIH

# Biochemistry

# &

# Microbiology

# Abstracts 6 - 38

EFFECTS OF LIGAND BINDING ON THE STABILITY AND DEAMIDATION OF VARIOUS ENZYMES

G.E. Gibson, K.Ü. Yüksel and R.W. Gracy, Dept. of Biochemistry, UNT/TCOM, Ft. Worth, Tx. 76107, USA.

Proteins are proposed to be degraded by the 'molecular wear and tear' or 'use it or lose it' mechanisms. The first theory proposes that enzymes will be worn out faster when they are catalytically active. The second hypothesis indicates that when ligands are bound to proteins they will be protected from denaturation and degradation. Previous studies in our laboratory have suggested that ligand binding to triosephosphate isomerase (EC 5.3.1.1, TPI) enhances the specific deamidation of $Asn^{71}$, leading to degradation of the enzyme. Thus, TPI seems to be an example of the 'wear and tear' mechanism.

Studies have been initiated to determine the effects of ligand binding on the stability of various enzymes which contain potential deamidation sites, including glucose-6-phosphate isomerase, alanine amino-transferase, fructose diphosphate aldolase, alcohol dehydrogenase, and phosphofructokinase. In each experiment, an enzyme is incubated at 50° C for a time period of five half-lives in the presence or absence of substrate, and the activities are measured periodically in order to determine a difference in the loss of activity between the two samples. The appearance of negatively charged deamidation products (Asn to $Asp^-$) is monitored by non-denaturing polyacrylamide gel electrophoresis. Our new data on glucose-6-phosphate isomerase indicate that ligands protect this enzyme from thermal denaturation. These experiments should establish a trend in ligand binding effects on enzymes that will aid in our understanding the mechanisms of protein degradation *in vivo*.

[Supported by grants from the National Institutes on Aging (AG01274) and The Texas Advanced Research and Technology Program (#2147)]

## COMPARATIVE STRUCTURAL STUDIES ON WILD TYPE AND MUTANT RECOMBINANT LCAT

Sulabha Paranjape,Tun-San Wen, G.S. Rao and Andras Lacko. Department of Biochemistry and Molecular Biology Texas College of Osteopathic Medicine/ University of North Texas

Comparative structural studies on purified plasma LCAT and recombinant LCAT (r-LCAT) were carried out. The molecular weight (67,000) and carbohydrate content (~ 23% by weight) of r-LCAT were identical to that of the human plasma enzyme. The fluorescence and circular dichroism spectra for these enzymes were very similar indicating little if any differences in their respective gross conformations. Comparative studies were carried out utilizing a human mutant (Fish eye disease LCAT) as a model. In this mutant form of the enzyme, Threonine123 is replaced by isoleucine resulting in marked changes in lipoprotein specificity. The wild type enzyme prefers HDL as substrate while the Thr $_{123}$—»Ile mutant prefers LDL as substrate. The circular dichroism spectra of of the wild type and the mutant LCAT showed a differences suggesting changes in α-helix structure. The changes in spectral properties in the presence of increasing concentration of guanidine HCL suggest that the tertiary structure of the wild type enzyme is more resistant to denaturation than the mutant enzyme. Preliminary studies resulted in the formation of r-LCAT crystals not yet suitable for X-ray analysis.

CARBOHYDRATE COMPONENTS OF RECOMBINANT LCAT. Geetha Sunderrajan, and Andras Lacko, Department of Biochemistry and Molecular Biology, Texas College of Osteopathic Medicine/University of North Texas, Ft. Worth, TX.

We have recently established a BHK (Baby Hamster Kidney) cell line which constitutively expresses significant quantities of human, recombinant LCAT (r-LCAT). The culturing of the transfected cells in a " cell factory" enabled the efficient production of large quantities of r-LCAT in the serum free medium. The r-LCAT preparations are purified in a single step, with nearly quantitative yield. The primary culture of BHK transfected cells produced sialylated form of r-LCAT whose sialic acid content as estimated by sialic acid assay is comparable with that of native human plasma LCAT. After passing through about two passages, these cells starts produce the desialylated form of r-LCAT as confirmed by chemical analysis and NMR studies. The absence of sialic acid in desialylated r-LCAT is apparently due to presence of a sialidase perhaps of lysozomal origin. We are currently investigating the conditions required for the production of fully sialylated forms of r-LCAT. A Sialidase inhibitor 2,3 dehydro-2-desoxy-N-acetyl-Neuraminic acid is being employed to suppress the sialidase secreted by the BHK cells. Physical/chemical characterization studies on the desialylated and fully sialylated enzyme forms are in progress.

**DETECTION OF GTP-BINDING PROTEINS ASSOCIATING WITH INSULIN SECRETORY GRANULES .** Adnan Dibas and Richard Easom .
Department of Biochemistry and Molecular Biology , Texas College of Osteopathic Medicine\University of North Texas , Fort Worth , 76107

GTP-binding proteins are involved in signal transduction in numerous pathways . Previous studies have demonstrated that nonhydrolyzable GTP-analogues stimulate insulin secretion from isolated pancreatic islets suggesting a putative role for GTP-binding proteins in this process .

In the present study , the hypothesis that GTP-binding proteins are present on the secretory granules of pancreatic β-cells was tested . Secretory granules were isolated from pancreatic islets and cultured β-cells (RINm5F) by established procedures employing stepped percoll gradients . By western blot analysis using antibodies raised against the GTP-binding site of Gα , three proteins of approximate molecular weights Mr = 60-66 KDa , Mr = 32 KDa and 20-24 KDa were detected . These data suggest the presence of at least one GTP-binding protein on the β-cell secretory granules . Further experiments are being conducted to determine the identity of these G-proteins .

**ALLOXAN-INDUCED SUPPRESSION OF INSULIN SECRETION: EVIDENCE FOR A ROLE OF $Ca^{2+}$-CALMODULIN-DEPENDENT PROTEIN KINASE-II (CAMPKII) IN INSULIN SECRETION.** Robert M. Wenham, Michael Landt and Richard A. Easom, Fort Worth, TX, and St. Louis, MO.

Alloxan, a potent diabetogenic agent, completely suppresses glucose-induced insulin secretion and concomittantly inhibits CamPKII activity. Alloxan, however, also inhibits glucokinase, a enzyme proposed to play a prominent role in glucose recognition by the β-cell. In order to probe for a role of CamPKII in insulin secretion, the ability of alloxan to suppress secretion induced by glyceraldehyde, whose metabolism by the β-cell is not dependent on glucokinase and $K^+$, which increases intracellular $Ca^{2+}$ and bypasses glucose metabolism, was asessed. Alloxan (562.5 μM) suppressed insulin secretion induced by glyceraldehyde and $K^+$ by 61% and 47% respectively. By contrast, insulin secretion induced by TPA, whose insulinogenic activity is dependent primarily on the activation of protein kinase C, was only modestly inhibited by alloxan. These data suggest that alloxan-induced suppression of glucose-induced insulin secretion is mediated at least in part by an inhibtion of CamPKII and provide further evidence for a positive role for this enzyme in insulin secretion.

## ROLE OF MYOSIN LIGHT CHAIN KINASE (MLCK) IN SECRETAGOGUE-INDUCED INSULIN SECRETION

Steven M. Walters, Mark C. Jones and Richard A. Easom
University of North Texas/Texas College of Osteopathic Medicine
Denton/Fort Worth, Texas

The principal response of the pancreatic β-cell to glucose stimulation is an increased intracellular Ca2+ concentration mediated through membrame depolarization and subsequent influx of Ca2+ through votage-dependent Ca2+ channels. However, the mechanism by which an increased Ca2+ concentration is translated into insulin release is not known. The present study addresses the hypothesis that Ca2+ -induced insulin secretion is mediated by the activation of a Ca2+ -calmodulin-dependent enzyme, myosin light chain kinase (MLCK). The presence of MLCK, approx. Mr=135kDa, in isolated islets was established by Western blot analysis using a non-muscle anti-chicken gizzard MLCK antibody. MLCK activity was also detected in islet homogenates and was completely inhibited by the MLCK inhibitor, KT5926 (100nM). Using a perifusion model, glucose-induced insulin secretion was markedly suppressed by 30 nM KT5926. K+ at 40-56 mM and 5-10 min. induced the activation of MLCK as indicated by an increased (~2-fold) incorporation of 32Pi into a 20kDa myosin light chain (MLC-20) immunoprecipitated from islet homogenates using an anti-human platelet myosin antibody. These data support a possible role of the activation of MLCK in secretagogue-induced insulin secretion.

**AUTOREGULATION OF CSF-1 EXPRESSION IN C-FMS TRANSFECTED HUMAN MONOBLAST U937 CELLS.** Mu-ya Liu, Department of Microbiology and Immunology and Ming-chi Wu, Department of Biochemistry and Molecular Biology, Texas College of Osteopathic Medicine Fort Worth, Tx 76107

The human monoblast cell line U937 can be induced by Phorbol 12-myristic 13-acetate to undergo differentiation. This treatment is accompanied by the expression of macrophage colony-stimulating factor (CSF-1). In order to study the mechanism of action of CSF-1, a CSF-1 receptor gene (c-fms) was transfected into U937 cells. Exogenous CSF-1 treatment induced an autocrine response of CSF-1 expression in this CSF-1 sensitive system. The time course for the induction of endogenous CSF-1 gene expression by exogenous CSF-1 was determined and all events were shown to be time dependent. CSF-1 stimulation of U937 cells also enhanced proto-oncogene c-jun and c-myc gene expression in the transfected cells. complementary DNA coding for Jun or Fos was introduced into U937 cells by transfection. The transfection did not generate a high level of CSF-1 gene expression which suggests that Fos and Jun alone are insufficient to induce CSF-1 synthesis.

**Immunolocalization of Basic Fibroblast Growth Factor During the Peri-implantation Period in the Mouse.** Robert J. Wordinger, Tonuia Jackson and I-Fen Chang, Dept. of Anatomy and Cell Biology, Univ. of North Texas, Texas College of Osteopathic Medicine, Fort Worth, Texas.

Fibroblast growth growth factors (FGF) constitute a family of related polypeptides which play an important role in physiological processes (e.g. cell proliferation, nerve cell differentiation, angiogenesis, wound healing, embryonic development). Basic FGF (bFGF) is one of the most characterized members of the family. Basic FGF may be a critical regulatory factor which acts to modulate embryo-endometrial interactions during implantation and decidualization. The objective of this experiment was to compare and contrast the immunohistochemical localization of bFGF during the peri-implantation period in the mouse. Pregnant mice were sacrificed on day 5, 6, 7 or 8 of gestation. Implantation sites were dissected and placed in Bouin's fixative. Paraffin embedded sections were exposed to primary antisera made in rabbits against (1) human recombinant bFGF or (2) amino acids 1-24 of the synthetic fragment of bovine bFGF (Andrew Baird, Whittier Institute, La Jolla, CA.). Sections were subsequently exposed to biotinylated goat anti-rabbit IgG and biotin-avidin-peroxidase complex. Specificity controls included (a) substitution of normal rabbit sera for the primary antisera, (b) omitting the primary antisera or (c) extracting sections with 2.0 M NaCl prior to the immunochemical procedures. No binding of the antibody was observed with any of the specificity control sections. Both the commercial antisera and the donated antisera against amino acids 1-24 resulted in identical localization patterns in the study. At day 5 the primary decidual zone and the surface and glandular epithelium associated with the non-decidualized endometrium is devoid of bFGF. Undifferentiated endometrial stroma and the basal lamina associated with epithelium were positive for bFGF. By day 6 large multinucleated decidual cells from the antimesometrial zone were surrounded by bFGF but lacked intracellular localization. Giant trophoblast cells were devoid of bFGF localization. By day 7 and 8 cells forming the cords of the intermediate zone exhibited diffuse intracellular bFGF localization. Endothelial cells lining the blood sinusoids were negative. Occasional large, ovoid cells exhibited intense localization of bFGF. Decidual cells of the mesometrial zone were surrounded by bFGF.

**Purification and Biochemical Characterization of Recombinant Human IL-8.** X-Q Kang, J.A. Wiggins, Q. Chen and S.R. Grant. Texas College of Osteopathic Medicine\University of North Texas, Fort Worth, TX 76107.

The cDNA for the human chemotactic interleukin, IL-8, was subcloned from a bacterial source into the eucaryotic vector expression system, baculovirus. Recombinant human IL-8, rhIL-8, was synthesized and secreted from Sf9 cells derived from Spodoptera frugiperda following infection of a recombinant virus harboring the full length IL-8 structural gene. Infected Sf9 cells produced rhIL-8 in a range from 0.5 to 2.0 mg of rhIL-8/liter of post infection cell culture media. The recombinant interleukin was purified (> 600 fold) to electrophoretic homogeneity using preparative HPLC. rhIL-8 retained all of the physical, immunological, and biochemical properties observed for the natural product, monocyte derived IL-8. rhIL-8 was assessed for biological efficacy by three criteria: a) ability to induce chemotaxis in human neutrophils, b)ability to induce oxygen burst metabolism, and c)ability to be recognized by purified rabbit antibody generated against monocyte derived IL-8. Antibody generated against monocyte derived IL-8 recognized rhIL-8 isolated during all stages of the purification protocol. rhIL-8 was strongly chemotactic for human neutrophils and exhibited a chemotactic index comparable to that reported for other strong chemotactic peptides. rhIL-8 was identified as a single silver stained band following SDS-PAGE having an estimated molecular weight of 9.2 kDa and displayed amino acid residue molar abundance homology predicted for the mature form of the interleukin. Baculovirus vector expression coupled to preparative HPLC proved to be a very efficient method for large scale recombinant interleukin production. Purified rhIL-8 will be used to identify and biochemically characterize a $G_{\alpha i}$ coupled IL-8 receptor signal transduction mechanism(s) involving an unidentified serine/threonine kinase.

**EXPRESSION OF HUMAN INTERLEUKIN-6 IN INSECT CELLS BY A BACULOVIRUS VECTOR.** Swati Tripathy, Mu-ya Liu, Zhang-Qui Wu, Fu-Mei Wu and Ming-chi Wu, Department of Biochemistry and Molecular Biology, Texas College of Osteopathic Medicine/University of North Texas, Fort Worth, Tx 76107

The Baculovirus Expression Vector System (BEVS) has been used to express more than 50 different genes. Recombinant proteins have been produced at levels ranging from 1 mg/L to 600 mg/L. The focus of this research is to express human interleukin-6 (1L-6) gene in insect cells, using Autographa californica nuclear polyhedrosis virus (AcNPV) as an expression vector. To construct the pVL1393-1L-6 recombinant virus, the 1L-6 cDNA was inserted into the baculovirus polyhedrin plasmid pVL1393. A new construct (pVL1393-1L-6) was obtained which contains the h1L-6 gene in the proper orientation downstream of the strong polyhedrin promoter. Supercoiled pVL1393-1L-6 DNA was subsequently cotransfected with wild-type AcNPV viral DNA into cell lines from the Fall Army worm Spodoptera frugiperda (Sf9). In vivo recombination events yielded a small population of recombinant viruses with the H1L-6 sequences incorporated into the original viral genome. This pVL1393-1L-6 chimeric viral isolate was identified and purified through a procedure involving successive rounds of plaque hybridization. By assaying the culture medium, it was demonstrated that recombinant virus infected Sf9 cells expressing h1L-6 which stimulates the proliferation of 1L-6 dependent B9 cells. Recombinant h1L-6 has apparent molecular weight of 21 Kda as shown in western blot analysis. Similar to our previous studies, the recombinant h1L-6 can stimulate the dispersed colony formation of rat monoblast leukemia MIA C-51 cells. At higher concentration, it also inhibits the proliferation of MIA C-51 cells. These results demonstrate that h1L-6 can be produced by Insect cells - Baculovirus expression system with immunological characteristics and biological activity identical to 1L-6 produced in animal cells.

**PROTEIN F1(GAP-43): ANTIBODIES AGAINST IT C-TERMINUS PEPTIDE WITH A NOVEL *IN VITRO* PHOSPHORYLATION SITE OF SERINE 209.** Hassan M. Azzazy and Ming-chi Wu, Department of Biochemistry and Molecular Biology, Texas College of Osteopathic Medicine, Fort Worth, Tx and Guenter W. Gross, Department of Biology Science, University of North Texas, Denton, Tx.

Protein F1 (GAP-43, B-50, neuromodulin, P-57), a neuron-specific calmodulin-binding phospho-protein enriched in the growth cones of elongating neurites, is correlated with long term potentiation (a model of synaptic plasticity), neuronal development, and neurotransmitter release. In this study, a 21-mer peptide (AKPKES*ARQDEGKEDPEADQE) that corresponds to the C-terminus of protein F1 (from position 204-224) was synthesized and used as an immunogen to produce anti-protein F1 antibodies. The antibodies showed good results in western blot analysis and in immunoprecipitation of $^{32}$P-phosphorylated protein F1. This result demonstrates that the produced anti-protein F1 antibodies can recognize both phosphorylated and unphosphorylated protein. The synthesized F1 peptide was phosphorylated *in vitro* by protein kinase C as shown from the HPLC profile and autoradiogram of F1 phosphopeptide. Thus serine 209 can be considered as a novel phosphorylation site for protein kinase C although its *in vivo* role remain to be established. The anti-protein F1 antibodies was also used to stain mouse spinal cord neurons in culture. This result clearly demonstrated that protein F1 is located exclusively in neurons but not in the glial cells.

PROTEIN SEQUENCING OF POSTTRANSLATIONALLY MODIFIED PEPTIDES and PROTEINS. K.Ü. Yüksel*, S.M. Mische, L.M. Mende-Mueller, P. Matsudaira, D.L. Crimmins, and P.C. Andrews. Assoc. Biomolecular Resource Facilities; *Biopolymer Analysis Laboratory, Department of Biochemistry and Molecular Biology TCOM.

To provide its members with opportunities to educate and evaluate themselves, ABRF prepares, distributes and evaluates analysis of unknowns. ABRF-92SEQ provided enough sample (500 pmol) for sequencing and other analyses, and incorporated post-translationally modified amino acids, and some standard problem regions [doublets, hydrophobic region, and deamidation site]:
ARGUAGGSAK JQQDRHPAVL TNGMGSEQEA KIHNFAK[37]
(U= PO4-Ser, J= Hpo). It contained alanines for repetitive yield calculations, and cleavage sites for CNBr, trypsin, endoproteinases V-8 and Asp-N.

The most correctly identified amino acid was Ala at residues 5 and 9 (100%). P-Serine was the most difficult amino acid to identify (13.9% accuracy), mostly misidentified as Ser or Cys. Hpo was less of a problem (77% accuracy), most often misidentified as His. There were no perfect sequence identifications for ABRF-92SEQ. Two facilities had all residues correct, except for residue 4, with one correct tentative identification of phosphoserine, and one misidentification as serine. Two others had the same shortcomings, plus they overcalled the peptide by one residue. The most complete sequence analysis reported used both sequence analysis and mass spectrometry to identify the modified amino acids, and reduction/alkylation with 4-vinyl pyridine to rule out cysteine at residue 4. To partially alleviate the problem of identifying modified PTH-amino acids, the ABRF is compiling data on their chromatographic identification.

## INTERCONVERSION OF THE TWO CONFORMATIONS OF TRIOSEPHOSPHATE ISOMERASE MONITORED BY $^{31}$P-NMR.

K. Ü. Yüksel, K.D. Schnackerz and R. W. Gracy, Dept. Biochemistry, Tx. Coll. Osteopathic Med. / U. North Tx., Ft. Worth, TX. 76107, USA.

The homodimeric enzyme triosephosphate isomerase (EC 5.3.1.1; TPI) from rabbit, chicken and yeast, treated with the substrate analogue 3-chloroacetol phosphate (CAP), exhibits two $^{31}$P-NMR resonances (5.4 & 6.2-6.6 ppm). In the presence of guanidine a single resonance is observed (4.5 ppm). Upon removal of the deanturant only the 5.4 ppm signal is restored. Previously denatured / renatured TPIwhen subsequently reacted with CAP also exhibits two $^{31}$P-NMR resonances with identical chemical shifts as the native protein. When native yeast CAP-TPI is incubated at 39 °C, the 6.2 ppm resonance disappears in a time dependent fashion. No addtional resonances are observed.

These data suggest that (a) the renatured enzyme can still be trapped in two different conformations by CAP, (b) these conformations are readily interconvertible, (c) the 5.4 ppm resonance represents the conformation of lower potential energy, and (d) an energy barrier must be overcome to attain this state.

This work was supported by grants from the NIH (AG01274), the Robert A. Welch Foundation (B-0502), and TX Advanced Research Fund (1247).

RELATIONSHIP OF THE CATALYTIC SITE AND PRIMARY DEGRADATION SITE OF TRIOSEPHOSHATE ISOMERASE.

A.-O. Sun, K. Ü. Yüksel, K. D. Schnackerz, and R. W. Gracy, Mol. Aging Unit, Dept. Biochem. & Mol. Biology, Univ. N. Tex., Tex. Coll. Osteop. Med., Ft. Worth, TX 76107, USA.

Triosephosphate isomerase (TPI) is the best characterized housekeeping enzyme of glycolysis and a prototype for the study of the initial events of protein degradation. We are exploring the relationship between the catalytic center and the degradation site by a combination of NMR, CD, and stability studies on the native dimer and heterodimers. Substrate binding or covalent reaction of the active site Glu165 with the substrate analogue 3-chloroacetol-phosphate (CAP) enhances the specific deamidation of Asn71 in the subunit interface, thereby destabilizing the dimer. Heterodimers from different species or from native and CAP-modified subunits have been formed and their distribution and stability examined. The distribution of dimers is not directly proportional to their stability, suggesting that at least two steps are involved in the interactions between the subunits. Deamidated CAP-TPI is readily hydrolyzed *in vitro* by either fibroblast extracts or by subtilisin. The site of the initial cleavage is the Thr139-Glu140 peptide bond near the hinged lid which folds over the catalytic center upon substrate binding. Following subtilisin-cleavage, the peptides remain noncovalently attached and the protein is catalytically active. Comparison of NMR, CD, catalytic and stability data of the heterodimers and parent homodimers supports the concept of molecular wear and tear. (Supported by a MERIT Award from the NIA, and grants from the Alexander von Humboldt Foundation, and the TX Advanced Technology and Research Fundation).

# REFOLDED HOMO- AND HETERODIMERS OF TRIOSEPHOSPHATE ISOMERASE: STRUCTURAL AND KINETIC CHARACTERIZATION.

A.-O. Sun, K. Ü. Yüksel and R. W. Gracy, Dept. Biochemistry, U. North Tx. / Tx. Coll. Osteopathic Med., Ft. Worth, TX. 76107, USA.

Chemically denatured globular proteins refold spontaneously, but structural rearrangements often take place leading to changes in molecular properties. The effects of reversible dissociation and denaturation on protein structure, stability, and catalytic properties of triosephosphate isomerase (EC 5.3.1.1; TPI) from rabbit and yeast were studied. Refolded TPI dimers were catalytically active, exhibited no aggregation or fragmentation, and comigrated with the native enzymes upon electrophoretic analyses. NMR and CD spectroscopy, on the other hand, indicated differences in structure. These differences were manifested as increased lability (denaturation and loss of activity) upon exposure to denaturans. Active site titration with the substrate analogue 3-chloroacetol phosphate showed one reactive site per subunit for both native and renatured enzymes, but the refolded dimers exhibited lower substrate and inhibitor binding affinity, and decreased catalytic efficiency (Kcat/Km). Thus, while the dimer can be easily dissociated, unfolded and reassembled into active dimers, the resultant dimers possess significant structural and catalytic differences.

This work was supported by grants from the NIH (AG01274), the Robert A. Welch Foundation (B-0502), and TX Advanced Research Fund (1247).

**STRUCTURE - FUNCTION RELATIONS IN *ASCARIS SUUM* PHOSPHOFRUCTOKINASE: EFFECTOR STUDIES.** G. S. Jagannatha Rao, Paul F. Cook, and Ben G. Harris. Department of Biochemistry, Texas College of Osteopathic Medicine, Fort Wort, TX-76107

Fluorescence and circular dichroism measurements show that *Ascaris suum* phosphofructokinase is activated by the positive effectors, Fructose 2,6-$P_2$ and AMP through specific and similar conformational changes. The enzyme is activated by both these effectors, in 20 mM phosphate buffer, pH 6.6 with 0.2 mM ATP and 1 mM F6P. The $K_{act.}$ values for AMP and F2,6$P_2$ are 25 ± 3 μM and 1.5 ± 0.2 μM, respectively. Both effectors quench enzyme tryptophan fluorescence in phosphate buffer, pH 6.6 in a concentration dependent manner. The $K_d$ values determined from the decrease in emission intensity at 342 nm as a function of effector concentration are 24 ± 3 μM for AMP and 1.0 ± 0.15 μM for F2,6$P_2$, in excellent agreement with the values of $K_{act}$. Both effectors also produce dramatic changes in CD spectrum of the enzyme in 20 mM phosphate buffer, pH 6.6, in the region from 240 to 190 nm representing the peptide backbone. calculations show an increase in α-helical content in the presence of either effector. The $K_d$ values obtained from the concentration dependence of the decrease in ellipticity at 210 nm are 22.8 ± 5.3 μM and 1.3 ± 0.2 μM, respectively, for AMP and F2,6$P_2$. The data imply that activation of PFK by these effectors is concomitant with structural changes in the enzyme. Further, comparison of the difference CD spectra for the effects of AMP and F2,6$P_2$ show that these two effectors produce similar conformational changes and probably stabilize a similar final activated state of the enzyme. Other hexose phosphate analogues like F6P, G1,6$P_2$ and FBP do not affect the CD spectrum of the enzyme.

**STRUCTURE - FUNCTION RELATIONS IN *ASCARIS SUUM* PHOSPHOFRUCTOKINASE: PH-EFFECTS.** G. S. Jagannatha Rao, Paul F. Cook, and Ben G. Harris. Department of Biochemistry, Texas College of Osteopathic Medicine, Fort Wort, TX-76107

The technique of circular dichroism has been used to probe the conformational changes accompanying pH-dependent allosteric transitions in the *Ascaris suum* phosphofructokinase. The enzyme displays ATP-inhibition, cooperative kinetics and hysteretic behavior below pH 7, but gradually loses these regulatory properties at higher pH. This change in kinetic behavior is associated with gross conformational changes as shown by pronounced shifts in the CD spectrum of the enzyme in the pH range 6 - 8. These pH-induced structural alterations are distinct from those caused by the effectors such as Fructose 2,6-bisphosphate and AMP. Both sedimentation equilibrium and gel filtration HPLC experiments show that the enzyme does not dissociate into dimers below pH 7 indicating that the observed pH-dependent CD-changes are not due to a shift in dimer/tetramer equilibrium, rather to conformational transitions within the tetramer. The pH-dependence of ellipticity at 210 nm gives a $pK_a$ of 6.4 ± 0.1 which is in agreement with the $pK_a$ of 6.8 ± 0.3 obtained from the loss of ATP-inhibition upon desensitization of the enzyme by chemical modification with diethylpyrocarbonate. The desensitized enzyme exhibits a pH-independent CD spectrum over the pH range 6-8. Results imply that pH-induced allosteric transitions observed for the *Ascaris suum* phosphofructokinase are the result of structural changes in the enzyme. The same residue, (probably histidine) that must be protonated for ATP-inhibition also serves as a trigger for these structural alterations. Thus the protonation state of a residue at or near the ATP-inhibitory site determines the enzyme conformation and whether ATP will inhibit by binding at the inhibitory site.

CHEMICAL MECHANISM OF 6-PHOSPHOGLUCONATE DEHYDROGENASE FROM *Torula*. Anthony J. Berdis* and Paul F. Cook#. Department of Biochemistry and Molecular Biology* and Department of Microbiology and Immunology#.
The pH dependence of kinetic parameters and dissociation constants for competitive inhibitors was determined in order to obtain information on the chemical mechanism for the 6-phosphogluconate dehydrogenase (6-PGDH) reaction from *Torula*. A mechanism is proposed in which an active site general base accepts the proton from the 3-hydroxyl concomitant with hydride transfer at C-3; the resulting 3-keto intermediate is decarboxylated to give the enol of ribulose 5-phosphate, followed by tautomerization of the enol to the keto product with the assist of a second enzyme residue acting as a general acid. There is also a requirement for an ionized phosphate of 6-phosphogluconate and ribulose 5-phosphate for optimum binding. Primary deuterium isotope effects upon V/K for 6-PG and NADP were obtained as a function of pH. Isotope effects on V/K are essentially independent of pH below pH 8 and decrease to approach unity at high pH. Comparison of the profiles obtained from the pH dependence of kinetic parameters with those profiles obtained for the pH dependence of isotope effects indicates that the pH and the isotope-dependent steps are different. Results are consistent with a mechanism in which a pH-dependent step precedes hydride transfer in which the hydroxyl of C-3 may be deprotonated prior to the hydride transfer that presumably produces the 3-keto-intermediate.
This work was supported by grants to PFC from NIH (GM 36799) and the Robert A .Welch Foundation (B-1031) and to AJB from Sigma Xi (GIAR 92023).

KINETIC MECHANISM OF O-ACETYLSERINE SULFHYDRYLASE-B. Chia-Hui Tai[1], Tony M. Jacobson [2]and Paul F. Cook[2]. Dept. of Biochemistry & Molecular Biology Texas College of Osteopathic Medicine and Dept. of Microbiology & Immunology, Fort Worth, TX 76107.

Initial velocity studies using both natural and alternative substrates suggest that OASS-B proceeds predominantly via a Bi Bi ping pong kinetic mechanism. The enzyme uses 5-thio-2-nitrobenzoate(TNB) as an alternative nucleophilic substrate. The presumed product S-(3-carboxy-4-nitrophenyl)-L-cysteine (S-CNP-Cys) was confirmed by $^1$H-NMR. The ping pong mechanism is corroborated by a qualitative and quantitative analysis of product and dead-end inhibition. Product inhibition by acetate is S-parabolic noncompetitive with partial substrate inhibition by OAS induced by high acetate concentrations. These data are consistent with acetate reversing the first half reaction and producing more free enzyme to which acetate may also bind. In addition, OAS can bind with a much weaker affinity to E:acetate and generate the α-aminoacrylate intermediate. Thus, there may be some randomness to the mechanism at high concentrations of the nucleophilic substrate. In addition, the kinetic mechanism for both isozymes with TNB as the reactant gives apparent substrate activation as the concentration of TNB is increased. UV-visible spectra of OASS-B exhibit absorbance maxima at 280 and 412 nm. Addition of OAS to enzyme shifts the absorbance maximum from 412 to 470 nm, with a pH independent extinction coefficient over the pH range 6 to 9.5, indicating the formation of the α-aminoacrylate intermediate. The OASS-B was also shown to catalyze an OAS deacetylase activity at pH 9.5.

This work was supported by grants to PFC from NSF (DMB 8912053), Robert A. Welch Foundation (B-1031), and NATO (900519).

**CRYSTALLIZATION AND PRELIMINARY X-RAY DATA FOR O-ACETYL SERINE SULFHYDRYLASE FROM *SALMONELLA TYPHIMURIUM*.** G. S. Jagannatha Rao, T. Jacobson, J. Mottonen, E. J. Goldsmith, and P. F. Cook. Department of Microbiology & Immunology, Texas College of Osteopathic Medicine, Fort Worth, TX-76107/UT Southwestern Medical Center, Dallas, TX-75235

O-Acetylserine sulfhydrylase is the second enzyme of cysteine biosynthetic pathway and catalyzes the formation of L-cysteine from sulfide and o-acetylserine. The reaction is an example of pyridoxal phosphate dependent β-elimination reactions. The enzyme has been purified to homogeneity from the enteric bacterium *Salmonella typhimurium* and has been crystallized in two different forms by hanging drop-vapor diffusion technique. One crystal form is in the hexagonal space group $P6_122$ with cell dimensions, a = b = 115 Å, c = 348 Å, $\alpha = \beta = 90°$ and $\gamma = 120°$. The unit cell contains two dimers of 68 kDa per asymmetric unit. The second crystal form is in the orthorhombic space group $P2_12_12_1$ with cell dimensions, a = 144 Å, b = 97 Å, c = 54 Å, $\alpha = \beta = \gamma = 90°$. The unit cell in this case contains two monomers of 34 kDa per asymmetric unit. Both forms diffract x-rays to better than 2.5 Å resolution and hence eminently suited for x-ray diffraction studies. A Complete native data set has been collected for the orthorhombic form and structure solution is in progress by direct methods as well as molecular replacement techniques. Elucidation of the three dimensional structure of this enzyme will provide insights into the catalytic function of the enzyme and facilitate a better understanding of pyridoxal phosphate catalysis in enzyme.

**SITE-DIRECTED MUTAGENESIS OF ACTIVE SITE RESIDUES OF THE GENE cysK ENCODING FOR O-ACETYLSERINE SULFHYDRYLASE A.** Vaishali D. Rege*, William E. Karsten**, Nicholas M. Kredich*** and Paul F. Cook**. * Dept. of Biochemistry, TCOM/UNT, Fort Worth, TX 76107. ** Dept. of Microbiology & Immunology, TCOM/UNT, Fort Worth, TX 76107. *** Dept. of Biochemistry, DUMC, Durham, NC 27710.

O-acetylserine sulfhydrylase-A (OASS-A) is a pyridoxal phosphate (PLP) dependent enzyme and catalyzes a reaction that produces L-cysteine from O-acetyl-L-serine and sulfide under aerobic conditions in *Salmonella typhimurium*. Studies on the kinetic and chemical mechanisms of OASS-A suggest the involvement of an active site lysine that forms Schiffs base with PLP. The enzyme with the change K42A shows no activity. The cysteine next to the Lys 42 is the only Cys in this protein. This Cys 43 was changed to Ala or Thr by site-directed mutagenesis. The changes in activities of C43A and C43T compared to the wild type enzyme suggest involvement of Cys 43 in catalysis. Also, the tryptophan residue at position 51, one of the two tryptophans present in the enzyme and is thought to be in the vicinity of the active site PLP was changed to Phe or Tyr. Further studies with these mutants would provide more information about the kinetic and chemical mechanisms of the enzyme.

This work was supported by grants to PFC from NSF (DMB8912053), Robert A. Welch Foundation(B-1031) and NATO (900519) and to NMK from NIH (DK12828) and (GM07184).

**PURIFICATION AND INITIAL VELOCITY STUDIES OF SERINE TRANSACETYLASE FROM *SALMONELLA TYPHIMURIUM*.** Lee-Shan Leu, Zhengzhang Pu and Paul F. Cook. Department of Microbiology and Immunology, Texas College of Osteopathic Medicine, Fort Worth, TX 76107.

Serine transacetylase (STA) is one of the two enzymes involved in the *de novo* synthesis of cysteine in enteric bacteria. STA catalyzes the transfer of an acetyl moiety from acetyl CoA to the β-hydroxyl of L-serine to generate the intermediate product O-acetyl-L-serine (OAS). STA has been purified from a $cys^-$ strain of *Salmonella typhimurium*, DW 18.1, and transformed with a multicopy plasmid, PRSM41, containing the gene for ampicillin resistance and the *cys* E gene. From 70 g of cell paste, approximately 35 mg of STA is obtained with final specific activity of about 50 units/mg. SDS-PAGE shows two closely spaced bands of about 40,000 MW and thses bands are also observed in native gels. The STA has been assayed at pH 7, 100 mM Hepes in the direction of OAS formation using the coupling of DTNB with the product, CoASH. In the direction of CoASH acetylation, the STA was assayed at pH 6, 100 mM Mes using the appearance of absorbance at 232 nm. An initial velocity pattern was obtained and it appears to intersect to the left of the ordinate consistent with a sequential kinetic mechanism. A repeat of the initial velocity pattern in the presence of 30 mM L-serine gives a series of parallel lines suggestive of a ping pong kinetic mechanism. The data of OAS production inhibition are consistent with an ordered addition of acetyl CoA prior to L-serine.

PRODUCT BINDING ENHANCES PYRIDOXAL PHOSPHATE FLUORESCENCE IN *O*-ACETYLSERINE SULFHYDRYLASE FROM SALMONELLA TYPHIMURIUM. G. David McClure, Jr. and Paul F. Cook. Department of Microbiology and Immunology, Texas College of Osteopathic Medicine, Fort Worth, TX 76107

Fluorescence spectroscopy was used to monitor binding of products of the enzymatic reaction to *S. typhimurium O*-Acetyl-L-serine sulfhydrylase-A (OASS-A), which catalyzes the formation of acetate and L-cysteine from *O*-acetyl-L-serine (OAS) and sulfide. One molecule of the cofactor pyridoxal 5'-phosphate (PLP) is bound to each apoenzyme protomer. The fluorescence emission spectrum of *S. typhimurium* OASS-A excited at 298 nm has maxima near 338 nm, due to tryptophan emission, and 500 nm, due to emission of PLP bound as Schiff base in holoenzyme. The 500 nm emission is enhanced in the presence of acetate or L-cysteine. Deprotonation of a distinct ionizable group on enzyme, with pK 7.2 for acetate and pK 8.0 for L-cysteine, is required for enhancement. Each of the acetate analogs, oxalate, trifluoroacetate, and propionate, elicits enhancement, suggesting that the carboxylate of acetate is important for binding. Either of the L-cysteine analogs, L-cystine or L-penicillamine, causes enhancement, consistent with a role for the amino or carboxylate group of L-cysteine in binding to enzyme. This work provides the first direct spectroscopic confirmation of the existence of complexes of OASS-A with each of the enzymatic reaction products, and provides insight into the nature of the binding sites for products in OASS-A.

**KINETIC AND CHEMICAL MECHANISM OF THE O-ACETYLSERINE SULFHYDRYLASE-A.** Srinivasa R. Nalabolu and Paul F. Cook. Texas College Of Osteopathic Medicine, Fort Worth, TX 76107.

The resonance stabilized quinonoid, 5-thio-2-nitrobenzoate (TNB) is a substrate for O-acetylserine sulfhydrylase-A (OASS-A) giving rise to the product S-(3-carboxy-4-nitrophenyl)-L-cysteine (S-CNP-Cys) as confirmed by ultraviolet-visible and 1H-NMR spectroscopy. A comparison of the kinetics of OASS-A indicates that the mechanism proceeds predominantly via a Bi Bi ping pong kinetic mechanism as suggested by an initial velocity pattern consisting of parallel lines at low concentrations of reactants, but competitive inhibition by both substrates as the reactant concentrations are increased. Product inhibition by acetate is S-parabolic noncompetitive. These data are consistent with acetate reversing the first half reaction and producing more free enzyme to which acetate may also bind. Thus, there may be some randomness to the mechanism at high concentration of the nucleophilic substrate. The acid-base chemistry of OASS-A requires a general base to remove a proton from the α-amine of OAS in the first half reaction. Either the same general base or the Schiff base lysine presumably acts to abstract the α-proton during the elimination reaction. In the second half reaction, there is a requirement for a general acid to protonate the α-carbon and for the active site lysine to be unprotonated.

This work was supported by grants to PFC from NSF (DBM 8912053), Robert A. Welch Foundation (B-1031), and Nato (900519).

**INHIBITION OF THE ADP-RIBOSE ELONGATION REACTION CATALYZED BY POLY(ADP-RIBOSE) POLYMERASE WITH AGMATINE-ADP-RIBOSE.**

Pacheco-Rodriguez, G. and Alvarez-Gonzalez, R. Depts. of Microbiology. & Immunol. and Biochem. & Mol. Biol. Texas College of Osteopathic Medicine; University of North Texas, Fort Worth, TX 76107-2699.

Poly(ADP-ribose)polymerase (**PARP**) [E.C.2.4.2.30] poly(ADP-ribosyl)ates several DNA binding proteins including itself (automodification) as well as histones proteins (heterologous modification). The successive transfer of ADP-ribose (ADPR) to a growing ADPR polymer may be studied by the use of mono(ADP ribosyl)ated molecules. We have synthesized Agmatine-(ADPR) with cholera toxin utilizing Agmatine and β-NAD as the substrates. This adduct inhibits the elongation activity of **PARP** at 2 μM NAD in the presence or absence of histones. The ADPR polymerization activity of **PARP** decreased from 3.6 to 1.9 in the absence of histones, from 0.40 to 0.21, and from 0.91 to 0.20 pmoles in the presence of either core histones or histone H1, respectively. When this inhibitor is added to the incubation reaction mixture at 200 μM, the size distribution of the polymers decreased from 6.22 to 4.38 in the automodification reaction, from 4.27 to 1.25 with core histones, and from 2.62 to 1.32 with histone H1 as determined by 20% PAGE. An increase in the percent of branching from 3.1 to 6.6 was observed in the presence of Agmatine-ADPR when Histone H1 was used as the modification target. In order to determine if this inhibition is due to the ADPR moiety or to the Agmatine moiety, reactions were carried out in the presence of Agmatine. Addition of Agmatine did not inhibit the ADP-ribose elongation activity of **PARP**; on the contrary, a sligth increase in the activity was exhibited ranging from 2 to 40 % with the different ADPR acceptors aforementioned. When rat liver chromatin was used as the poly(ADP-ribosyl)ation system, similar patterns of inhibition on the ADP-ribosylation elongation reaction were observed. Results obtained are consistent with the conclusion that the inhibitory effect is due to the ADPR covalentely linked to the guanidinium group of Agmatine. We propose that the inhibition is a competition between Agmatine-ADPR and the protein distal ADPR residue of the growing polymer. This would also demostrate for the first time that a second substrate binding site specific for the ADPR elongation acceptor is present in **PARP**.

Acnowledgement is made to the donors of the Petroleum Research Fund Administrated by the ACS.

**THE AUTOMODIFICATION REACTION OF POLY(ADP-RIBOSE) POLYMERASE OCCURS VIA A DISTRIBUTIVE MECHANISM.** Mendoza-Alvarez H., & Alvarez-Gonzalez R. Department of Microbiology & Immunology, Texas College of Osteopathic Medicine-University of North Texas Fort Worth, TX 76107-2699.

Poly(ADP-ribose)polymerase (PARP), a chromatin-bound and DNA-dependent enzyme [EC 2.4.2.30], modulates chromatin structure and function during DNA-strand breaking and rejoining by a post-translational auto-poly(ADP-ribosyl)ation reaction (automodification) utilizing βNAD as a substrate. Here, we have characterized the molecular mechanism of the automodification reaction with pure enzyme at nanomolar and micromolar concentrations of NAD. The electrophoretic mobility of automodified enzyme in pH 5.0 LDS-gels, was unaffected at nanomolar [NAD]. However, the electrophoretic mobility of automodified PARP significantly decreased as the concentration of NAD was increased from 10 mM to 200 mM. The size of enzyme-bound (ADP-ribose)n increased from predominantly monomeric to oligomeric as the NAD concentration was increased from 200 nM and 400 nM to 0.8 and 1.6 mM, respectively. By contrast, the size of ADP-ribose chains went from oligomeric to polymeric and highly branched as the NAD concentration was increased from 1 and 2 mM to 10, 50, 100 and 200 mM, respectively. In contrast, the size of ADP-ribose chains synthesized with pure enzyme at mM concentrations of NAD in the presence of 1 mM benzamide changed from exclusively monomeric to oligomeric, and subsequently, from oligomeric to highly branched molecules, as the ratio of [NAD]/[benzamide] was increased from 1/100 to 1/20 to 1/10 and 1/5, respectively. These results are consistent with the conclusion that the automodification reaction of PARP occurs via a distributive mechanism.

Acknowledgment is made to the donors of The Petroleum Research Fund, administered by the ACS for their support of this project.

**CHEMICAL STABILITY OF PROTEIN-(ADP-RIBOSE)n CHROMATIN CONJUGATES AT pH 9.0 AND pH 13.0 IN THE PRESENCE OR ABSENCE OF MAGNESIUM.**

Alvarez-Gonzalez R. and Mendoza-Alvarez H. Department of Microbiology & Immunology, Texas College of Osteopathic Medicine-University of North Texas Fort Worth, TX 76107-2699.

Poly(ADP-ribose)polymerase, histone H1, histone H2b, and a 42 kDa protein were radiolabeled following incubation of rat liver chromatin with [$^{32}$P] βNAD$^+$ as shown by LDS-PAGE. Addition of 1 mM benzamide completely inhibited this reaction. Thus, these proteins represent poly(ADP-ribose) and not mono(ADP-ribose) acceptors. Incubation of protein-(ADP-ribose)$_n$ conjugates in 0.1 N NaOH, 20 mM EDTA showed that histone H1 and H2b-(ADP-ribose)$_n$ were degraded with a half life of approximately 10 min. The half life of 42 kDa-(ADP-ribose)$_n$ was less than 10 min. These results are consistent with mono-ester linkages involving Glu and/or Asp residues as poly(ADP-ribosyl)ation sites. In contrast, over 30% of PARP-(ADP-ribose)$_n$ conjugates remained intact after 60 min of incubation suggesting that amino acid residues other than Glu and/or Asp are modified in the auto-poly(ADP-ribosyl)ation reaction of this enzyme. Experiments performed with PARP-(ADP-ribose)$_n$ conjugates generated with purified polymerase confirmed this interpretation. Interestingly, protein-free polymers were stable in 0.1 N NaOH, 20 mM EDTA for 3 hours at 60 °C. However, they were quantitatively hydrolyzed to PRAMP and 5'-AMP in the presence of 10 mM $MgCl_2$. These results suggest that poly(ADP-ribose)-magnesium complexes involving polymeric phosphoanhydride bonds are formed as intermediates of alkaline hydrolysis. Protein-(ADP-ribose)$_n$ chromatin conjugates were also synthesized in permeabilized SVT2 cells. Polymers generated in cultured cells appeared as triple radiolabeled bands upon electrophoresis on high resolution polyacrylamide gels following chemical release from protein at pH 9.0. Each triplet was found to be constituted of a mixture of the: *i)* intact; *ii)* 5'-phosphorylated; and *iii)* 5'-hydroxylated forms of free (ADP-ribose)$_n$.

Acknowledgment is made to the donors of The Petroleum Research Fund, administered by the ACS, and the VFW Auxiliary Cancer Research Fund for their support of this project.

**ADP-RIBOSE ELONGATION OF MONO(ADP-RIBOSE)-ARGININE METHYL ESTER BY POLY(ADP-RIBOSE)POLYMERASE.**

Pacheco-Rodriguez, G., Moss, J., and Alvarez-Gonzalez, R. Deptartment. of Microbiology. & Immunology. Texas College of Osteopathic Medicine-University of North Texas, Fort Worth, TX 76107-2699 and NHLBI, NIH, Bethesda, MD 20892.

Poly(ADP-ribose) polymerase (PARP) [E.C. 2.4.2.30] is a DNA-dependent enzyme that appears to catalyze the initiation, elongation, and branching reactions of protein-bound ADP-ribose polymer synthesis in mammalian chromatin. PARP is estimated to catalyze 40 rounds of ADP-ribose elongation for every branching step. It may also catalyze over 100 ADP-ribose polymerization reactions for every initiation event. To monitor the ADP-ribose elongation reaction, we synthesized [$^{32}$P] labeled ADP-ribose-arginine methyl ester[AME] with an avian arginine-specific mono(ADP-ribosyl) transferase using AME and [$^{32}$P]βNAD as substrates. Mono(ADP-ribosyl)-AME was purified by SAX-HPLC and boronate chromatography. Pure ADP-ribose-AME appeared to be an efficient ADP-ribose acceptor in the histone-dependent elongation reaction catalyzed by PARP with unlabeled βNAD as the ADP-ribose donor. Putative (ADP-ribose)-[$^{32}$P](ADP-ribose)-AME was identified by its slower electrophoretic mobility on 20% polyacrylamide gels. Incubation of the elongation reaction components in 0.2 N NaOH and 10 mM $MgCl_2$ for 3 h at 60 °C yielded a [$^{32}$P] radiolabeled product that co-migrated with [$^{32}$P] phosphoribosyladenosine monophosphate. Thus, it appears that AME-(ADP-ribose) can be used as an ADP-ribose acceptor in the elongation reaction catalyzed by PARP.

Acknowledgment is made to the donors of The Petroleum Research Fund administered by the ACS, and the VFW Auxiliary Cancer Research Fund for their support of this project.

**MOLECULAR CLONING AND CHARACTERIZATION OF THE SPORE PHOTOPRODUCT LYASE (*SPL*) GENE, WHICH IS INVOLVED IN REPAIR OF ULTRAVIOLET RADIATION-INDUCED DNA DAMAGE DURING SPORE GERMINATION.** Patricia Fajardo-Cavazos, Crescencio Salazar, and Wayne L. Nicholson, Department of Microbiology and Immunology, Texas College of Osteopathic Medicine, 3500 Camp Bowie Boulevard, Fort Worth, TX 76107.

Upon ultraviolet (UV) irradiation, *Bacillus subtilis* spore DNA accumulates the novel thymine dimer 5-thyminyl-5,6-dihydrothymine. Spores can repair this "spore photoproduct" (SP) upon germination either by the *uvr*-mediated general excision repair pathway or by an SP-specific pathway called *spl* involving *in situ* monomerization of SP to two thymines by an enzymatic activity named spore photoproduct lyase. Mutants lacking both repair pathways produce spores which are extremely sensitive to UV. In order to clone DNA which corrects a mutation in the *spl* pathway called *spl-1*, a library of *Eco*RI fragments of chromosomal DNA from *B. subtilis* strain 168 was constructed in the integrative plasmid pJH101 and was introduced by transformation into a mutant *B. subtilis* strain which carries both the *uvrA42* and *spl -1* mutations, and transformants whose spores exhibited UV resistance were selected by UV irradiation. Using a combination of genetic and physical mapping techniques, the DNA responsible for restoration of UV resistance was shown to be present on a 2.3 kb *Eco*RI-*Hin*dIII fragment which was mapped to a new locus in the *metC-pyrD* region of the *B. subtilis* chromosome immediately downstream from the *ptsI* gene. The *spl* coding sequence was localized on the cloned fragment by analysis of *in vitro*-generated deletions and by nucleotide sequencing. The *spl* nucleotide sequence contains an open reading frame capable of encoding a polypeptide of 40 kilodaltons which contains regional amino acid sequence homology to DNA photolyases from a number of bacteria and fungi. (Supported by grants from the Texas Advanced Research Program (009768-034) and the National Institutes of Health (GM47461) to W.L.N. C.S. was supported by a Project SEED Grant from the American Chemical Society.)

**Detection of Extracellular Enolase from *Candida albicans*.** P. Sundstrom and G.R. Aliaga. Department of Microbiology and Immunology. Texas College of Osteopathic Medicine. Fort Worth, TX 76107.

*Candida albicans* is an opportunistic pathogen that can cause severe disease in immunocompromised patients. Enolase of *C. albicans* has been shown to circulate in the blood of neutropenic cancer patients with disseminated candidiasis and is an immunodominant antigen. The presence of hematogenous *C. albicans* enolase raises questions regarding the mechanism of enolase release from fungal cells. Our previous experiments using a cDNA probe have shown that enolase mRNA is abundant in *C. albicans.* We performed experiments to determine if *C. albicans* enolase could be detected in culture supernatants of freshly grown yeast and hyphal forms. Extracellular enolase was detectable from unbroken cells by assaying for enzymatic activity and by immunoblotting. However, the amount of extracellular enolase was less than 0.5 % of the total cellular enolase activity and may have been derived from small numbers of inviable cells. To investigate whether other glycolytic enzymes are present outside of fungal cells we also assayed for the presence of glyceraldehyde-3-phosphate dehydrogenase (GAP-DH) activity. Whereas total cellular GAP-DH and enolase levels were similar, GAP-DH activity in hyphal supernatants was approximately 8-fold lower than that of enolase, and was not detected in yeast culture supernatants. In conclusion, the data suggest that *C. albicans* enolase is not actively secreted, but is present outside the cell in higher levels than GAP-DH.

**Characterization of enolase gene expression of *Candida albicans*.** P. POSTLETHWAIT* and P. SUNDSTROM. The University of North Texas, Denton, Texas and Texas College of Osteopathic Medicine, Ft. Worth, Texas.

*Candida albicans*, a dimorphic opportunistic fungal pathogen, colonizes mucous membranes in healthy individuals. Serious mucosal and/or systemic infections can occur when host defenses become impaired. Understanding mechanisms which regulate fungal growth are necessary for designing strategies to prevent infection. In yeast, glycolytic enzymes are the most abundant cellular proteins and their expression is tightly regulated depending upon environmental conditions. We have cloned and sequenced a cDNA for enolase of *C. albicans* and found high homology to *Saccharomyces cerevisiae* enolase genes. Enolase of *C. albicans*, which catalyzes the dehydration of 2-phosphoglycerate to yield phosphoenolpyruvate, is an abundant cellular protein and is also an immunodominant antigen in patients with disseminated candidiasis. Studies to determine the number of enolase genes, their transcriptional start sites, and steady-state mRNA levels during various growth conditions were performed. The existence of two tandemly repeated genes for *C. albicans* enolase was strongly suggested by Southern blot experiments. Northern and slot blot analyses were used to quantitate mRNA levels in yeast versus hyphal forms as well as during different phases of logarithmic growth. Primer extension experiments revealed two transcription start sites approximately 36 and 44 nucleotides upstream of the AUG initiation codon.

IDENTIFICATION AND MOLECULAR CHARACTERIZATION OF THE PLEIOTROPIC GENE *csrA* THAT AFFECTS GLYCOGEN GIOSYNTHESIS, GLUCONEOGENESIS, CELL SIZE AND SURFACE PROPERTIES IN *ESCHERICHIA COLI* K12. Mu Ya Liu, Min Gong, Anne Marie Brun, and Tony Romeo*. Texas College of Osteopathic Medicine, Fort Worth, TX 76107 / University of North Texas, Denton, TX 76203.

One of the metabolic pathways that is transcriptionally activated as *Escherichia coli* enters the stationary phase of growth is the glycogen biosynthesis pathway. In order to identify factors that regulate glycogen biosynthesis *in trans*, a collection of transposon mutants was constructed and was screened for mutations which alter glycogen accumulation and the expression of a plasmid-encoded *glgC'-'lacZ* fusion. The *trans*-acting glycogen-excess mutation TR1-5 was found to affect the expression of genes representative of two glycogen synthesis operons, *glgC* (ADPglucose pyrophosphorylase) and *glgB* (glycogen branching enzyme), and the gluconeogenic gene *pckA* (phosphoenolpyruvate carboxykinase). The gene that was mutated was designated *csrA*, for carbon storage regulator. The TR1-5 mutation affected cell size and surface (adherence) properties, and affected glycogen biosynthesis independently of cAMP, cAMP receptor protein and ppGpp, which positively regulate the expression of *glgCA*. The gene *csrA* was mapped to 58 min or 2834.8 kb on the genome. A plasmid clone of the native *csrA* gene strongly inhibited glycogen synthesis in all *E. coli* strains that were tested. Nucleotide sequence analysis, complementation and *in vitro* expression studies indicated that *csrA* encodes a 61 amino acid polypeptide. S1 nuclease mapping experiments demonstrated that regulation of *glgC* expression via CsrA was at the transcriptional level. The CsrA polypeptide has no known homologue, indicating that it belongs to a new class of genetic regulatory factors. This study provides further evidence that carbon storage in *E. coli* is intricately regulated via the expression of the *glgCA* genes.

**Lipopeptides of Potential Importance in *Mycobacterium avium* GPL Biosynthesis.**

E.R. Wright and W.W. Barrow. Texas College of Osteopathic Medicine, Fort Worth, Texas, 76107

Due to the importance of the *Mycobacterium avium* complex, studies using metabolic inhibitors and pulse-chase techniques were conducted to identify potential lipid precursors in GPL biosynthesis. Mycobacteria were allowed to incorporate [$^{14}$C]-phenylalanine ([$^{14}$C]Phe) and resulting radiolabeled lipids analyzed by thin-layer chromatography (TLC), high performance liquid chromatography (HPLC) and autoradiography. Previous studies have demonstrated that treatment of serovar 4 with 2-deoxy-D-glucose (2-DDG) results in the accumulation of at least three Phe-containing lipopeptides. In an effort to further study the role of these lipopeptides in GPL biosynthesis, pulse-chase experiments using [$^{14}$C]Phe and timed studies using different levels of 2-DDG were conducted. Analysis of autoradiographic profiles allowed visual tracking of radiolabel incorporation over time. HPLC separation and partial chemical analysis of selected radiolabeled components suggests that they represent intermediates in GPL biosynthesis. At least one of the Phe-containing lipopeptides isolated from these studies appears to be identical with a lipopeptide previously obtained from GPL-deficient rough mutants of serovars 4, 8, and 20.

# Cardiovascular

# Abstracts 39 - 63

**Increased Carotid Baroreflex Responsiveness During Sustained Nitroprusside Infusion.**

**X.R. Shi, J.T.Potts, C.G.Crandall, B.H.Foresman, and P.B.Raven.**

**Department of Physiology, Texas College of Osteopathic Medicine, Fort Worth, TX 76107.**

We compared the carotid baroreflex (CBR) function in six healthy young men after 20±2 min (mean±SE) of nitroprusside infusion (NI). NI increased ($p<0.05$) heart rate (HR) and decreased ($p<0.05$) mean radial arterial pressure (MAP) from the control 50±3 to 64±5 bpm and 91±1 to 83±2 mmHg, respectively. Changes in carotid sinus pressure (CSP) were generated by rapid neck pressure/suction (NP/NS). CBR function was assessed by HR-CSP and MAP-CSP curves using logistic modelling. During sustained NI, the calculated central point, threshold, and operating range (the difference between the saturation and threshold) of CSP were not significantly changed, though HR-CSP and MAP-CSP curves were shifted up-ward and down-ward to the left, respectively. However, the responding range of both HR and MAP (the difference between the maximum and minimum) was significantly increased by 7±2 bpm and 7±1 mmHg. These changes with NI increased HR-CSP gain from control 0.32±0.09 to 0.65±0.12 bpm/mmHg ($p<0.02$), and MAP-CSP gain from control 0.27±0.06 to 0.34±0.03 mmHg/mmHg ($p<0.136$). We conclude that during NI carotid baroreflex responsiveness was increased as a result of an increase in responding range.

**(supported by grant from NIH #43202 & AHA-TX Aff. #91G-146)**

AORTIC BARORECEPTOR-HEART RATE REFLEX RESPONSE TO HYPOTENSION: EFFECT OF FITNESS. X. Shi, C.G. Crandall, J.T. Potts, J.W. Williamson, B.H. Foresman, & P.B. Raven. Department of Physiology, Texas College of Osteopathic Medicine, Fort Worth, TX 76107.

In seven average fit (AF) men, aged 28±1.2 years, and five high fit (HF) men, aged 26±1.3 years, we compared their heart rate (HR) reflex response during sodium nitroprusside (SN) induced hypotension. Fitness level was assessed by determining maximal oxygen uptake ($VO_{2max}$) on a treadmill. $VO_{2max}$'s were 45.7±0.8 and 63.5±1.6 ml/kg/min in the AF and HF subjects, respectively, $p<0.001$. Steady state SN infusion decreased mean intra-radial arterial pressure (MAP) by 13mmHg in both groups, however, the increases in HR were significantly ($p<0.05$) less in the HF (15.7±4.0 bpm) than the AF (24.2±2.8 bpm). When neck suction (NS) was applied to counteract the decreased carotid sinus transmural pressure during steady state SN infusion, thereby isolating the aortic baroreceptors, the increased HR of the HF subjects averaged 6.9±2.8 bpm and in the AF subjects average 16.6±2.7 bpm, $p<0.02$. The calculated gains (from the ratio of the changes in HR to MAP) listed below:

| | | AF | (%) | HF | (%) | p value |
|---|---|---|---|---|---|---|
| SN | (bpm/mmHg) | 2.0±0.3 | (100) | 1.2±0.2 | (100) | 0.05 |
| SN+NS | (bpm/mmHg) | 1.3±0.3 | (65) | 0.5±0.1 | (37) | 0.02 |
| Diff. | (bpm/mmHg) | 0.7±0.2 | (35) | 0.7±0.1 | (63) | N.S. |

Diff. = SN minus SN+ NS.

These data suggest that the aortic baroreceptor-HR reflex is less responsive in the HF than the AF subjects.

**(supported in part by NIH grant #HL43202)**

AORTIC BAROREFLEX CONTROL OF HEART RATE FOLLOWING 15 DAYS SIMULATED MICROGRAVITY. Craig G. Crandall, Keith A. Engelke, Victor A. Convertino, Peter B. Raven. Texas College of Osteopathic Medicine, Fort Worth, TX 76107 and NASA, Kennedy Space Center, FL 32899.

To determine the effects of microgravity on the aortic baroreflex control of heart rate, we exposed seven male subjects (mean age 38±3 years) to 15 days bed rest in the 6° head-down position. Aortic baroreflex control of heart rate (HR) was determined during a steady-state phenylephrine (PE) induced increase in mean arterial pressure (MAP) of 15 mmHg, combined with lower body negative pressure (LBNP) to counteract central venous pressure increases, and neck pressure (NP) to offset the increased carotid sinus transmural pressure. The sensitivity of the aortic baroreflex was assessed by determining the ratio of the differences in HR to MAP ($\Delta$HR/$\Delta$MAP) between baseline and aortic baroreceptor isolated (PE+LBNP+NP) conditions. The $\Delta$HR/$\Delta$MAP ratios for each stage are illustrated below (mean±SEM, *$p<0.05$ between pre- and post-bed rest conditions).

| | PE | PE+LBNP | PE+LBNP+NP |
|---|---|---|---|
| Pre-bed rest | 0.69±0.08 | 0.72±0.16 | 0.45±0.07 |
| Post-bed rest | 0.86±0.10 | 0.83±0.24 | 0.84±0.18* |

Therefore, 15 days simulated microgravity exposure increases the sensitivity of the aortic baroreflex control of HR. This effect may prove beneficial in attenuating microgravity-induced orthostatic hypotension.

*(Support in part by NASA-NGT50751 and NAG9-611.BASIC grants)*

**NEUROGENIC PRESSOR REFLEX ELICITED WITH LOWER-BODY POSITIVE PRESSURE IN MAN.**

J.W. Williamson, B. Hanel*, P.B. Raven, J.H. Mitchell and N.H. Secher*. Department of Anaesthesia, Rigshospitalet, University of Copenhagen, Denmark.

The purpose of this study was to determine if the increase in resting mean arterial blood pressure (MAP) observed with the application of lower-body positive pressure (LBPP) involved a neurogenic reflex. Subjects (n=8) were fitted with medical anti-shock (MAS) trousers to provide LBPP. Cephalad translocation of fluid was prevented during LBPP with the use of upper-thigh cuffs inflated to a supra-systolic pressure of 300 torr. Epidural anesthesia (EA) was administered to block group III & IV afferent neural activity from the legs. Heart rate (HR), MAP (brachial artery), central venous pressure (CVP, direct line), and cardiac output (CO, thoracic electrical impedance) were recorded during LBPP before and after EA. Following inflation of the upper-thigh cuffs, the MAS trousers were inflated for two minute periods to pressures of 30, 60, and 90 torr. Before EA, MAP and diastolic blood pressure were elevated ($p<0.05$) at MAS trouser pressures of both 60 and 90 torr, with no changes ($p>0.05$) in HR, CO, or CVP. The $12.5\pm3.1\%$ and $16.6\pm4.4\%$ increases in resting MAP with LBPP of 60 and 90 torr, respectively, were blocked by the EA in both cases. These findings indicate the MAP increase was neurally mediated via muscle afferent activity. Furthermore, when LBPP of 90 torr was applied to only one leg, the pressor response was less ($p<0.05$) than that elicited from compression of both legs. In conclusion, we propose the existence of a neurogenic pressor reflex to LBPP in resting man which may be dependent upon changes in intramuscular pressure and the quantity of muscle mass compressed.

**Supported in part by the Forskeracademiet, Aarhus, Denmark**

CHRONIC SYMPATHECTOMY ALTERS FAT AND CARBOHYDRATE METABOLISM IN MYOCARDIUM. N.A. LONGLET, S.C. LEE, R.T. MALLET, M.L. HAMRICK, A. HEYMANN, AND C.E. JONES. Dept. of Physiology, Texas College of Osteopathic Medicine, Ft Worth, TX 76107.

Chronic ventricular sympathectomy elicits changes in the coronary circulation and in myocardial $O_2$ utilization, indicating changes in its metabolism. To test this hypothesis, we compared selected metabolic parameters between 4 week surgically sympathectomized dog hearts (S) and sham operated controls (C). Left ventricular tissue samples were quick frozen using an Alko biopsy drill. Relative to C, the following changes in S were noted (values are means ± SE,): There were significant increases ($p<0.05$) in the contents of glycogen (262.3±5.3 vs 196.6±5.9), fructose-1,6-diphosphate (0.192±0.021 vs 0.0892±0.019 μmol/gdry), lactate (6.22±0.53 vs 3.98±0.44 μmol/ gdry), and in the optimal activities of hexokinase (0.0323±0.004 vs 0.019±0.002 U/mg), phosphofructokinase (0.2310±0.017 vs 0.087±0.001 U/mg), and lactate dehydrogenase (7.01±0.39 vs 5.37±0.46 U/mg), as well as decreases in pyruvate (0.250±0.007 vs 0.338±0.014 μmol/gdry), dihydroxyacetone phosphate (0.088±0.01 vs 0.14± 0.01 μmol/gdry) and acetyl CoA (0.009±0.001 vs 0.016±0.002 μmol/gdry). There were decreases in the optimal activities of phosphorylase a (0.015±0.004 vs 0.0464±0.004 U/mg) and carnitine acyl transferase (0.016±0.001 vs 0.075±0.001 U/mg). There were no differences in the contents of high energy phosphates. These data suggest that chronic sympathectomy decreases the ability of the heart to utilize free fatty acids as a fuel source and this is balanced by increased capacity for glycolytic flux. (Supported by NIH HL-29232 and HL-07652.)

**$G_s$-Adenylyl Cyclase Coupling is Reduced in Chronically Sympathectomized Cardiac Ventricles.** Eugene Quist, Ranga Vasan, S-S. Lee, Brian Foresman, Patricia Gwirtz and Carl E. Jones. Texas College of Osteopathic Medicine, Fort Worth, TX

The effect of chronic ventricular sympathectomy on sarcolemmal; i) muscarinic receptor (MR) density ii) beta adrenoceptor (ßAR) density iii) adenylyl cyclase (AC) activity and iv) $G_s$ content was studied. Sarcolemma (SL) were isolated from the right and left ventricles of 7 control dogs (2 sham- and 5 non-operated) and 6 dogs with ventricles sympathectomized 4 weeks earlier. Membrane protein recovery and sarcolemmal $Na^+$+$K^+$-ATPase were not significantly different in tissues from control and sympathectomized animals. As a result of sympathectomy, the density of MRs as determined from [$^3$H]-QNB binding was decreased approximately 20 % in the left but not in the right ventricles. The density of ßARs as determined from [$^3$H]-CGP 12177 binding studies was unchanged in ventricular SL from control and sympathectomized hearts. In contrast, basal AC activity was approximately 40 % less in sympathectomized (151.9 ± 44 pmoles/mg/min) versus control (237 ± 20 pmoles/mg/min) ventricular SL. Isoproterenol, a ßAR agonist, stimulated AC activity 129 ± 26 % and 60 ± 6 %, respectively, in sympathectomized and control heart SL. However, maximal AC activity in the presence of $G_s$ (NaF) or AC ($MnCl_2$) stimulants was identical in SL from all groups. Furthermore, $G_{s\alpha}$ content estimated from optimal cholera toxin/ARF catalyzed ADP-ribosylation was 3.1 pmoles/mg in left ventricular SL from control and sympathectomized ventricles. Therefore alterations in AC or Gs content were not likely responsible for the reduction in AC activity in sympathectomized hearts. Therefore the reduced contractile function associated with chronic sympathectomy may be at least partially related to a reduction in $G_s$ coupling with AC.

**ADENOSINE DECREASES OXYGEN CONSUMPTION OF CONTROL AND ISOPROTERENOL STIMULATED MINCED CANINE MYOCARDIUM.** Z. Gao, S.-C. Lee, and H. F. Downey, Department of Physiology, Texas College of Osteopathic Medicine\University of North Texas, Fort Worth, TX 76107

The effect of adenosine on oxygen consumption ($MVO_2$) of minced myocardium from six pentobarbital anesthetized dogs was studied. Myocardium was cut into 0.2 mm x 0.6 $mm^2$ pieces with a McIlwian tissue chopper and suspended in modified Krebs solution. Four aliquots from each heart containing approximately 15 mg myocardium were treated as follows: Control; Adenosine ($10^{-6}$ M); Isoproterenol ($10^{-5}$ M); Adenosine ($10^{-6}$ M) plus Isoproterenol ($10^{-5}$ M). $MVO_2$ was determined from the steady rate of decrease in $PO_2$ of tissue placed in a Diamond Electro-Tech oxygen chamber at 37°C. $PO_2$ was measured with a Diamond Electro-Tech Chemical Microsensor and linear recorder. The following $MVO_2$ (nmol $O_2$/mg protein/min) were measured: Control 0.36 ± 0.03; Adenosine 0.29 ± 0.03; Isoproterenol 0.52 ± 0.05; Isoproterenol plus Adenosine 0.46 ± 0.05. $MVO_2$ differed significantly ($P < 0.05$) between 1) Control and Adenosine, 2) Control and Isoproterenol, 3) Isoproterenol and Isoproterenol plus Adenosine. The results demonstrate that adenosine decreases myocardial oxygen consumption under basal conditions and also partially antagonizes the effect of isoproterenol on oxygen consumption of minced canine myocardium. (Supported by NIH grant HL-35027.)

SIZE-DEPENDENT RESPONSIVITY OF ISOLATED CANINE CORONARY ARTERIES TO ENDOGENOUS VASOACTIVE SUBSTANCES. J.B. Parker, M.L. Hamrick, S.C. Lee, R.J. Sinclair, and C.E. Jones. Dept. of Physiology, Texas College of Osteopathic Medicine, Fort Worth, Texas 76107.

The responses of canine coronary arteries of various sizes to adenosine and acetylcholine were studied. Isolated arteries ranging from 61-1,240 μm lumen diameter were mounted in a Halpern vessel chamber, and the lumen was pressurized to 40 mmHg with zero flow. Lumen diameter, wall thickness, and total diameter were determined using a Living Systems video dimension analyzer and recorded on a Grass strip recorder as well as on video tape. Maximal vessel diameter ($D_{max}$) was first determined using $Ca^{++}$ free physiological saline containing 1% albumin. KCl was then used to constrict each vessel to approximately 50% $D_{max}$ before determination of the adenosine and acetylcholine responses. Maximal vasodilation caused by adenosine in large arteries (> 450 μm) was 82.7 ± 0.41% (S.E.) of $D_{max}$ which was significantly less ($P<0.05$) than the 91.82 ± 0.32% seen in small arteries (< 350 μm). Furthermore, the $ED_{50}$ for adenosine in large arteries (0.204 ± 0.003 μM) was significantly greater than in small arteries (0.030 ± 0.006 μM). There was a clear transition zone between lumen diameters of 350-450 μm. The maximal vasodilatory response to acetylcholine was also diameter dependent. For large arteries, the maximal response was 90.39 ± 0.11% of $D_{max}$, while for small arteries the response declined to a value of 82.37 ± 2.52% . This difference was sadistically significant. Thus, our data suggest that responses to both adenosine and acetylcholine are size-dependent in canine coronary arteries. Responses to other endogenous vasoactive substances are now being examined. (Supported by NIH grants HL-29232 and HL-07652.)

**PYRUVATE-ENHANCED CYTOSOLIC ENERGETICS PARALLELS FUNCTIONAL RECOVERY IN POSTISCHEMIC CANINE MYOCARDIUM.** RT Mallet, W Fan, T Iwamoto and HF Downey. Texas College of Osteopathic Medicine\University of North Texas, Fort Worth, TX 76107.

Pyruvate (5-10 mM) markedly increases left ventricular contractile function and cytosolic phosphorylation potential in isolated, Krebs-Henseleit + glucose perfused, working guinea pig hearts 'stunned' by global low-flow ischemia (*Eur J Biochem 180*: 221-233, 1989). The present study tested whether pyruvate could produce similar improvements in blood-perfused, *in situ* heart following regional ischemic stress. Twelve pentobarbital-anesthetized mongrel canines were enrolled in the study. Contractile dysfunction was produced by six 5 min LAD occlusions with intervening 10 min reflows. Regional function in the left anterior descending (LAD) coronary perfusion territory was assessed from segmental shortening as a percentage of pre-occlusion baseline (SS) measured with piezoelectric crystals implanted in the midmyocardium. Beginning at 30 min reflow, 10 mM intracoronary pyruvate was infused into the LAD; in six controls, NaCl was infused at a similar rate. Collateral blood flow (ml · g tissue$^{-1}$) during prior occlusion, quantitated with radioactive microspheres, did not differ between the two treatment groups (pyruvate: 0.172 ± 0.042; NaCl: 0.176 ± 0.044). Effects of pyruvate and NaCl on SS were taken as the difference between treatment and pre-treatment baseline and expressed as a percentage of pre-occlusion level (ΔSS). ATP, creatine phosphate (CrP) and creatine (Cr) were measured in stop-frozen myocardium at 15 min treatment; CrP/Cr was taken as an index of cytosolic phosphorylation potential. Results (±SE) are as follows (heart rate (HR), min$^{-1}$; dP/dt, mm Hg · s$^{-1}$, ΔSS, % baseline, {ATP}, μmol · g dry mass$^{-1}$; *: $P < 0.05$ *vs.* NaCl):

| Treatment | HR | $dP/dt_{max}$ | $dP/dt_{min}$ | ΔSS | {ATP} | CrP/Cr |
|---|---|---|---|---|---|---|
| **Pyruvate** | 143 | 2090 | -2180 | 61* | 22.1 | 1.73* |
| | ±12 | ±380 | ±160 | ±15 | ±1.4 | ±0.17 |
| **NaCl** | 145 | 2050 | -2490 | -9 | 21.2 | 0.90 |
| | ±14 | ±430 | ±440 | ±23 | ±1.6 | ±0.25 |

Thus, 10 mM pyruvate increased regional function and energetic state in postischemic *in situ* myocardium (AHA TX Affil. 92G-155).

## THE IMPORTANCE OF RIGHT ATRIAL PRESSURE IN DETERMINING CORONARY FLOW.

Sheng Wang, Carl E. Jones, Konrad W. Scheel, Sue E. Williams, Kim D. Chen, John K. Schofield.
Department of Physiology, Texas College of Osteopathic Medicine, Fort Worth, TX 76107

Previous reports have suggested that elevated left ventricular end diastolic pressure impedes left coronary blood flow. However, in those experiments elevated ventricular pressure was accompanied by elevated right atrial pressure. The present experiments were designed to determine the independent effects of left ventricular end diastolic pressure (LVEDP), and right atrial pressure (RAP) on coronary flow. We used a blood perfused, beating, isolated dog heart preparation. A saline filled balloon was attached to a vertical tube and inserted into the left ventricle. During maximum dilation of the coronary arteries with adenosine, LVEDP was raised from 2 to 20 mmHg, while RAP was maintained at 0 mmHg. In separate experiments, RAP was raised from 0 to 20 mmHg while LVEDP was maintained at 2 mmHg. During both procedures coronary perfusion pressure remained constant at 100 mmHg, and late diastolic coronary flows were recorded. At a LVEDP of 20 mmHg, left coronary flow was decreased by only 2.2 ± .63 % compared to control flow ($p>0.05$). In contrast, at a right atrial pressure of 20 mmHg, left coronary flow was reduced significantly by 17 ± 2 % ($p<0.05$). We conclude that RAP is a more important determinant of coronary flow than LVEDP.

(Supported by: Am. Heart Assoc., Texas Affiliate and NIH grants HL-35030 and HL-29232).

**CORONARY PRESSURE-FLOW AUTOREGULATION PROTECTS MYOCARDIUM FROM PRESSURE-INDUCED CHANGES IN OXYGEN DEMAND.** X.-J. Bai, T. Iwamoto, A. G. Williams, JR., W.-L. Fan and H. F. Downey. Texas College of Osteopathic Medicine\University of North Texas, Fort Worth, TX 76107.

Pressure-flow autoregulation (PFAR) minimizes changes in coronary blood flow (CBF) when coronary perfusion pressure (CPP) is altered. A positive effect of CPP on myocardial oxygen consumption ($MVO_2$, Gregg's phenomenon) has been noted under some conditions, and is thought to result from CPP-induced changes in coronary vascular volume (CVV). In this investigation the effect of CPP on CVV and $MVO_2$ was examined as a function of the potency of PFAR. In 11 anesthetized dogs the LAD was cannulated and perfused at CPPs from 60 to 180 mmHg. CVV was computed from the transit time of i.c. injected $^{51}Cr$-labeled red blood cells and CBF. Regional arterial-venous oxygen content was measured, and $MVO_2$ computed. Autoregulatory closed-loop gain (Gc) was computed, and the data analyzed according to whether GC was greater than 0.4 (PFAR present) or less than 0.4 (PFAR poor or absent). Effects of CPP on CVV and $MVO_2$ are shown in the Table.

| | Gc > 0.4 | | Gc < 0.4 | |
|---|---|---|---|---|
| | Slope | P | Slope | P |
| CVV | .03 ml/100g/mmHg | < .05 | .12 ml/100g/mmHg | < .001 |
| $MVO_2$ | .002 ml/min/100g/mmHg | NS | .04 ml/min/100g/mmHg | < .001 |

CVV was more sensitive to changes in CPP when PFAR was absent. $MVO_2$ was sensitive to changes in CPP only when PFAR was absent. We conclude that PFAR protects myocardium from CPP-induced changes in CVV and $O_2$ demand. (Supported by NIH grant HL35027)

**HIGH-FLOW ISCHEMIA PRECONDITIONS CANINE MYOCARDIUM AGAINST SUBSEQUENT ISCHEMIA.** T. Iwamoto, X.-J. Bai, A. G. Williams, Jr., and H. F. Downey. Department of Physiology, Texas College of Osteopathic Medicine\University of North Texas, Fort Worth, TX 76107.

A brief period of ischemia or hypoxia has been reported to protect myocardium from infarction during subsequent, sustained ischemia. To determine whether a period of high flow energy demand/supply imbalance would limit myocardial infarct size, 15 anesthetized dogs were subjected to 5-min stimulation of the stellate cardiac nerve 10 min before 60-min occlusion of the left circumflex artery (LCX) followed by 5-hr reperfusion. In STIM-R group a pneumatic occluder was partially inflated to prevent an increase in LCX flow. In STIM group flow was allowed to increase freely by approximately two-fold. Control group received no stimulation. Infarct size (IS) and area at risk (AAR) were determined by triphenyl tetrazolium chloride staining and Evans blue dye, respectively. Collateral blood flow (MBF) was measured with radioactive microspheres. Dogs with more than 20% of normal flow to the inner two-thirds of the ischemic region were excluded. Hemodynamic values and MBF were comparable among all groups. IS, as a percentage of AAR and as a function of MBF, was significantly lower in the STIM-R than in the control group, but IS was not lower in the STIM group. Thus, energy supply/demand imbalance without flow reduction preconditioned myocardium against subsequent ischemia. Increased energy demand alone did not produce preconditioning. (Supported by NIH grant HL-35027.)

**ADENOSINE DECREASES OXYGEN CONSUMPTION OF CONTROL AND ISOPROTERENOL STIMULATED MINCED CANINE MYOCARDIUM.**

Z. Gao, S.-C. Lee, and H. F. Downey.
Department of Physiology, Texas College Osteopathic Medicine\University of North Texas, Fort Worth, TX 76107

The effect of adenosine on oxygen consumption ($MVO_2$) of minced myocardium from six pentobarbital anesthetized dogs was studied. Myocardium was cut into 0.2 mm x 0.6 $mm^2$ pieces with a McIlwian tissue chopper and suspended in modified Krebs solution. Four aliquots from each heart containing approximately 15 mg myocardium were treated as follows: Control; Adenosine ($10^{-6}$ M); Isoproterenol ($10^{-5}$ M); Adenosine ($10^{-6}$ M) plus Isoproterenol ($10^{-5}$ M). $MVO_2$ was determined from the steady rate of decrease in $PO_2$ of tissue placed in a Diamond Electro-Tech oxygen chamber at 37°C. $PO_2$ was measured with a Diamond Electro-Tech Chemical Microsensor and linear recorder. The following $MVO_2$ (nmol $O_2$/mg protein/min) were measured: Control 0.36 ± 0.03; Adenosine 0.29 ± 0.03; Isoproterenol 0.52 ± 0.05; Isoproterenol plus Adenosine 0.46 ± 0.05. $MVO_2$ differed significantly ($P < 0.05$) between 1) Control and Adenosine, 2) Control and Isoproterenol, 3) Isoproterenol and Isoproterenol plus Adenosine. The results demonstrate that adenosine decreases myocardial oxygen consumption under basal conditions and also partially antagonizes the effect of isoproterenol on oxygen consumption of minced canine myocardium. (Supported by NIH grant HL-35027.)

**EFFECTS OF SNUFF ON BLOOD FLOW TO PANCREAS OF THE ANESTHETIZED DOG.** A. G. Williams, Jr., K. D. Huckabee, M. M. Muncy, T. Barnes, and H. F. Downey. Department of Physiology, Texas College of Osteopathic Medicine\University of North Texas, Fort Worth, TX 76107.

We have demonstrated pronounced vasoconstrictory action of nicotine in the pancreas (J. Pharmacol. Exp. Ther. 216:363-367, 1981). In this investigation, experiments were conducted on dogs anesthetized with morphine-alpha chloralose to examine the effects of snuff on blood flow and vascular conductance in the pancreas. Pancreatic blood flow was determined from tissue trapping of differently labeled 15$\mu$m radioactive microspheres injected into the left ventricle under control conditions and with snuff in the right buccal cavity. Ventilation was held constant to avoid chemoreceptor-activated lung inflation reflexes. Results:

| Dose (g/kg) | n | AoP (mmHg) | Flow (ml/min/g) | Conductance (% change) |
|---|---|---|---|---|
| 0.0000 | 41 | 136±3 | 0.52±0.05 | -- |
| 0.0031 | 6 | 146±9 | 0.34±0.07 | -24±12 |
| 0.0062 | 7 | 158±10 | 0.39±0.07* | -12±1* |
| 0.0125 | 7 | 154±14 | 0.38±0.06 | 0±4 |
| 0.0250 | 7 | 171±11* | 0.47±0.11* | -46±12* |
| 0.0500 | 7 | 186±15* | 0.27±0.07* | -63±7* |
| 0.1000 | 7 | 213±14* | 0.08±0.02* | -91±2* |

AoP = Mean aortic pressure. * = P > 0.01 vs respective control values.

Snuff, at doses of 0.0062 g/kg and greater, reduced pancreatic blood flow and vascular conductance, despite an increase in aortic blood pressure. (Smokeless Tobacco Research Council, Inc. grant #0313.)

**EFFECTS OF NICOTINE ON REGIONAL BLOOD FLOW IN THE CHEEK AND TONGUE OF ANESTHETIZED DOGS.** K. D. Huckabee, M. M. Muncy, A. G. Williams, Jr., and H. F. Downey. Department of Physiology, Texas College of Osteopathic Medicine\University of North Texas, Fort Worth, TX 76107

We previously reported hyperemia in oral tissues exposed to snuff and vasoconstriction in other oral tissues. Experiments were conducted on six anesthetized dogs to examine the effects of nicotine on regional blood flow in the right and left cheek mucosa (RC and LC) and right and left sides of the tongue (RT and LT). Blood flow (ml/min/g) was determined with radioactive 15 $\mu$m microspheres injected into the left ventricle under control conditions and during application of nicotine (40 or 80 $\mu$g/kg in the right buccal cavity). Mean aortic pressure (AoP) was 148±6 mmHg pre-nicotine, 163±6 mmHg during low dose nicotine, and 175±18 mmHg during high dose nicotine. Vascular conductance (ml/min/g/mmHg) was determined to examine vascular responses independent of changes in AoP. Data (mean±SE) are shown in table.

| Tissue | Pre-Nicotine Flow | Nicotine Low Dose %▲Conductance | Nicotine High Dose %▲Conductance |
|---|---|---|---|
| RC | 0.11±.02 | 454±55* | 440±256 |
| LC | 0.12±.02 | -8±2* | -46±12* |
| RT | 0.16±.03 | 113±76 | 350±154 |
| LT | 0.16±.03 | 9±20 | -18±17 |

A significant (*P<0.05) hyperemia occurred in cheek mucosa exposed directly to nicotine, whereas significant vasoconstriction occurred in the contralateral cheek mucosa. Effects of nicotine on tongue were variable but tended to follow effects observed in cheek mucosa. Nicotine appears responsible, at least in part, for the effects of snuff on regional oral blood flow (Supported by Smokeless Tobacco Research Council grant 0313.)

CARDIAC OPIOIDS: EFFECTS OF VENTRICULAR DENERVATION AND EXERCISE. Barbara A. Barron, Lawrence X. Oakford, John F. Gaugl, Nancy Longlet, Carl E. Jones, Patricia A. Gwirtz, James L. Caffrey. Departments of Physiology and Anatomy and Cell Biology, Texas College of Osteopathic Medicine, Ft Worth, TX 76107

Our data clearly indicates that enkephalins originate in cardiomyocytes. Frozen tissue sections were incubated with an antibody to Met-enkephalin-arg-phe (ME-ap) and a fluorescent-labelled second antibody. The antibody crossreacts with peptide B and proenkephalin which contain ME-ap at their carboxyl terminal ends. The fluorescence is observed in ordered lines perpendicular to the longitudinal axis of the myocyte, concentrated around the intercalated disc, suggesting an opioid function in communication between cells or an unique secretory mechanism which utilizes the intercalated disc to export peptides. The fluorescence was absent from control sections. Proenkephalin content measured with the same antibody is more than 6 times greater in the ventricle than the atria (130 vs 24 fmol/mg protein). However, ME immunoreactivity (ir) is uniformly distributed throughout the myocardium (2.5 fmol/mg protein). This differs from the catecholamines, which are more concentrated in the atria and further supports the localization of enkephalins in the myocardium as well as in cardiac nerves.

Dog ventricles were surgically denervated or sham-operated and tissue collected 4 weeks later. Denervation produced the expected decrease in ventricular catecholamine content and also decreased atrial norepinephrine concentration. Proenkephalin-ir was unchanged by denervation however the product, ME, was decreased in the denervated ventricles (1.5 fmol/mg protein). Exercise decreased both norepinephrine and ME concentrations in cardiac tissue without affecting epinephrine or proenkephalin. This indicates that neuronal input to cardiomyocytes regulates processing and/or release of enkephalin.

Supported by American Heart Assoc. TX 91A-165 and NIH HL 29232.

CARDIAC OPIOIDS: EFFECTS OF VENTRICULAR DENERVATION AND EXERCISE. Barbara A. Barron, Lawrence X. Oakford, John F. Gaugl, Nancy Longlet, Carl E. Jones, Patricia A. Gwirtz, James L. Caffrey. Departments of Physiology and Anatomy and Cell Biology, Texas College of Osteopathic Medicine, Ft Worth, TX 76107

Our data clearly indicates that enkephalins originate in cardiomyocytes. Frozen tissue sections were incubated with an antibody to Met-enkephalin-arg-phe (ME-ap) and a fluorescent-labelled second antibody. The antibody crossreacts with peptide B and proenkephalin which contain ME-ap at their carboxyl terminal ends. The fluorescence is observed in ordered lines perpendicular to the longitudinal axis of the myocyte, concentrated around the intercalated disc, suggesting an opioid function in communication between cells or an unique secretory mechanism which utilizes the intercalated disc to export peptides. The fluorescence was absent from control sections. Proenkephalin content measured with the same antibody is more than 6 times greater in the ventricle than the atria (130 vs 24 fmol/mg protein). However, ME immunoreactivity (ir) is uniformly distributed throughout the myocardium (2.5 fmol/mg protein). This differs from the catecholamines, which are more concentrated in the atria and further supports the localization of enkephalins in the myocardium as well as in cardiac nerves.

Dog ventricles were surgically denervated or sham-operated and tissue collected 4 weeks later. Denervation produced the expected decrease in ventricular catecholamine content and also decreased atrial norepinephrine concentration. Proenkephalin-ir was unchanged by denervation however the product, ME, was decreased in the denervated ventricles (1.5 fmol/mg protein). Exercise decreased both norepinephrine and ME concentrations in cardiac tissue without affecting epinephrine or proenkephalin. This indicates that neuronal input to cardiomyocytes regulates processing and/or release of enkephalin.

Supported by American Heart Assoc. TX 91A-165 and NIH HL 29232.

**MET-ENKEPHALIN-ARG-PHE (MEAP) INHIBITS VAGAL CONTROL OF HEART RATE.** J.L. Caffrey, B.A. Barron, Z. Mateo and J.F. Gaugl. Department of Physiology, Texas College of Osteopathic Medicine, University of North Texas, Fort Worth, TX 76107.

We have extracted several proenkephalin derivatives from the dog myocardium. A large portion of these peptides crossreact strongly with a C-terminal directed MEAP antibody. Since MEAP represents the C-terminal proenkephalin sequence, the antibody also recognizes proenkephalin and a number of intermediate fragments as well. The MEAP activity in the heart is 30X higher than met-enkephalin and is concentrated five-fold higher in the ventricles than in the atria. Immunofluorescent labeling of the myocardium with this antibody produces a pattern of fluorescent lines perpendicular to the myocytes over the area of the intercalated discs. A group of dogs were treated with atenolol and the right vagus was stimulated at 0.5, 1, 2, and 4 Hz. This produced a graded decrease in heart rate between 10 and 50 bpm. MEAP was then infused into the left ventricular chamber at rates between 30 and 3000 pmol/kg/min and after three minutes the vagal stimulations were repeated. MEAP reduced the vagal response by 60%. An $ED_{50}$ was apparent at 300 pmol/kg/min which provides an $EC_{50}$ of about 3 nM. The MEAP-mediated suppression of the vagus was completely blocked by the high affinity opiate antagonist diprenorphine (100 $\mu$g/kg). These data strongly suggest that local myocardial enkephalins actively inhibit vagal input to the heart. Supported by NHLBI 33380 and TCOM organized research.

MET-ENKEPHALIN-ARG-PHE (MEAP) OPPOSES VAGAL CONTROL OF THE HEART PROXIMAL TO THE MUSCARINIC RECEPTOR. Z. Mateo, L.D. Napier, B. Henderson, B.A. Barron, J.F. Gaugl and J.L. Caffrey. Department of Physiology, Texas College of Osteopathic Medicine, Fort Worth, TX

Pro-enkephalin-like immunoreactivity (PE) has been extracted from canine myocardium. PE activity in ventricular tissues was several times higher than that found in comparable atrial extracts. MEAP, the C-terminal sequence of PE, decreased the negative chronotropic effect of vagal stimulation when administered intra-arterially. The following experiments were conducted to determine whether MEAP exerts its effect distally by interacting with acetylcholine (ACH) at the cardiomyocyte or proximally by interfering with the release of ACH. The muscarinic agonist, methacholine, was introduced into the left ventricular inflow in short, 15 second infusions. The infusions were adjusted to produce a graded decrease in heart rate comparable to that obtained during vagal stimulation. Competitive adrenergic innervation to the heart was surgically eliminated by severing the ansa subclavia bilaterally and through pretreatment with atenolol. Heart rate response to increasing vagal stimulation and increasing methacholine were evaluated first during infusion of vehicle, saline with 0.1% ascorbic acid. After recovery, the responses were evaluated again during the infusion of MEAP (3 nmoles/min/kg). During vehicle infusion both vagal stimulation and methacholine produced graded decreases in heart rate. Subsequent introduction of MEAP reduced the vagal effect by more than 50%. By contrast the negative chronotropic effect of methacholine was largely unaltered by the peptide infusion. These data suggest that the effect of MEAP on vagal function is mediated at a site proximal to the muscarinic receptor. MEAP may accomplish this by reducing the release of ACH either from post-ganglionic axon terminals in the sinoatrial node or from preganglionic axon terminals in the adjacent epicardial parasympathetic ganglia.

**THE EXTRACTION AND SEPARATION OF CIRCULATING ENKEPHALINS IN THE DOG.** L.D. Napier, Z. Mateo, B. Henderson, B.A. Barron, J.F. Gaugl and J.L. Caffrey. Department of Physiology, Texas College of Osteopathic Medicine, Fort Worth, TX.

Several larger products of the proenkephalin gene (proenkephalin, Peptide-B and met-enkephalin-arg-phe) are nearly 30X more concentrated in the dog heart than the commonly assayed met-enkephalin. Met-enkephalin-arg-phe (MEAP) appears to have significant biological activity regulating the parasympathetic control of the heart. To determine the role of the peptides in the heart and to characterize their action, they need to be efficiently extracted from the blood while protecting them from further degradation and processing. Prior to assay, the peptides must also be separated from one another since the available assay is unable to distinguish among them. The following describes efforts to optimize procedures for extracting and separating the peptides. Initially, the peptides were radiolabelled with $^{125}I$ to facilitate this process. Extraction procedures were evaluated by mixing radioactive peptide and whole blood. The initial strategy consisted of rapid cooling by dilution with cold saline and acidification. Several acids have been evaluated including acetic, citric and tricarboxylic. The red cells and plasma were separated by high speed centrifugation at 4°C and the recovery of peptide in the supernatant was determined. The recovery of radioactivity in the supernatant after cold dilution alone was greater than 80%. Experience suggests, however, that most of the biological activity will have been degraded. TCA provided rapid removal of both red cells and most plasma proteins. The recovery of acid soluble peptides in the supernatant, however, was less than 20%. Citric acid appears to offer an intermediate solution with 72% recovery of added MEAP after centrifugation. Complete evaluation of the extraction procedure will necessarily require chromatographic verification of the recovered peptide by HPLC. Since the peptides in question differ significantly in size, less analytic chromatographic procedures are being evaluated to separate extracted peptides prior to assay. These include several forms of gel filtration, ion exchange and selective adsorption. In this regard, simple separation on Sephadex G-50 followed by concentration on C-18 SPE cartridges holds some promise.

## QUANTITATIVE IN-VIVO STUDY OF THE CORONARY EPICARDIAL ARTERIAL PRESSURE-VOLUME RELATIONSHIP

Dan Manor, Rona Shofti, Samuel Sideman, Rafael Beyar
Heart System Research Center, Department of Biomedical Engineering, Technion-Israel Institute of Technology, Haifa 32000 Israel, and Department of Physiology, Texas College of Osteopathic Medicine, Fort Worth, TX 76107

Coronary arterial occlusion is associated with a decrease in the distal coronary pressure, with retrograde systolic flow waves. The objects of this study were to examine the arterial pressure-volume relationship and the mechanical properties of the vessels' wall under conditions of proximal occlusion. The study was carried out in 7 anesthetized mongrel dogs. The proximal part of the left anterior descending (LAD) artery was totaly occluded for approximately 60 [sec], and the distal LAD flow and pressure were recorded. The results yield that the flow in the distal LAD oscillates around the zero level. Integration of the flow signal with respect to time yields the intraluminal arterial volume changes in the region between the location of occlusion and the flowmeter. The relationship of the LAD pressure vs. volume changes over one cardiac cycle exhibits significant hysteresis loop. The area bounded by the hysteresis loop corresponds to the energy lose (W) due to the distension of the arterial wall, while the dynamic arterial distensibility ($C_{dyn}$) can be calculated from the ratio of the volume to pressure excursions. Mean work and compliance per unit arterial length were found to be 12.63±8.25 [erg $cm^{-1}$]and 1.13±0.73 [ml $mmHg^{-1}$ $cm^{-1}$ $x10^{-4}$], respectively. These results represent the first estimates of the *in vivo* mechanical properties of the arterial wall under low pressure conditions.

(Supported by: Women's Division of the American Technion Society (NY) and partially supported by the Anna and George Ury Research Fund (Chicago, IL) and the Adelaide and Michael Kennedy-Leigh Fund (London, UK))

VALIDATION OF THE COSMED K2 PORTABLE TELEMETRIC OXYGEN UPTAKE ANALYZER.

S.L. Taylor, C.G. Crandall, P.B. Raven. Dept. of Physiology, Texas College of Osteopathic Medicine, Fort Worth, TX 76107.

The purpose of this study was to assess the accuracy of the Cosmed K2 telemetric oxygen uptake analyzer. Fifteen subjects performed two maximal graded exercise tests (GXT); one using the K2 and the other using our standardized breath-by-breath (BBB) system. Heart rate (HR) and oxygen uptake ($\dot{V}O_2$) were obtained at each stage of a Bruce protocol GXT. The subjects' HRs were not significantly different at any stage between the two GXTs. As the table of means±sem illustrates, $\dot{V}O_2$ measured with the K2 apparatus was significantly different from the $\dot{V}O_2$ measured with the BBB system at stage 1, while no differences were observed at stages 2, 3, 4, or 5. When the respiratory quotient correction factor (C1K2) was used to account for the inherent error of the K2 system lacking a $CO_2$ analyzer, no differences in $\dot{V}O_2$ remained between the two systems at any stage of the GXT.

| | Stage 1 | Stage 2 | Stage 3 | Stage 4 | Stage 5 |
|---|---|---|---|---|---|
| BBB | 18.9±0.5 | 24.2±1.8 | 34.4±0.7 | 45.4±1.3 | 57.6±2.2 |
| K2 | 17.1±0.6* | 22.6±0.5 | 33.6±0.7 | 46.9±1.4 | 61.8±2.6 |
| C1K2 | 17.7±0.6 | 23.2±0.5 | 34.2±1.0 | 45.6±1.6 | 60.5±2.8 |

Oxygen uptakes in ml/kg/min. BBB - Breath-By-Breath system; K2 -Cosmed K2; C1K2 - $\dot{V}O_2$ after using the respiratory quotient correction factor of the K2; (*significantly different than the value obtained from the BBB system for that stage $p<0.05$).

We conclude the K2 accurately measures oxygen uptake at all stages of the GXT when an appropriate correction factor is used.

*(Supported by NASA/JSC: Grant #s NAG-9-420, and NAG-9-507)*

**ELEVATED RIGHT ATRIAL PRESSURE DECREASES, PRIMARILY, RIGHT CORONARY FLOW AND GENERATES ARRHYTHMIAS.**

John Schofield, Konrad W. Scheel, Sue E. Williams, James B. Parker.
Department of Physiology, Texas College of Osteopathic Medicine, Fort Worth, TX.

The purpose of this study was to determine the effects of elevated right atrial pressure on both, coronary hemodynamics and electrical activity. Six dog hearts were studied on an isolated, beating, blood perfused heart system in which the coronary perfusion pressure was maintained constant at 100 mmHg. Coronary flows to the left anterior descending (LAD), left circumflex -, (LCX), right -, and septal artery were simultaneously monitored during elevation of right atrial pressures by venous outflow restriction. After the venous pressure stabilized, LAD, LCX, right, and septal flows were reduced to 35 ± 12 %, 32 ± 12 %, 15 ± 9 %, and 24 ± 12 % of control flow, respectively. After restriction of venous outflow, right atrial pressure rose to 74 ± 16 mmHg in 35 ± 4 sec, and arrhythmias occurred after right atrial pressure had risen to 19.7 ± 2.3 mmHg. We conclude that an elevated right atrial pressure exerts its greatest effect on reducing right coronary perfusion, probably because of a reduction in perfusion pressure gradient and stretching of myocardial wall (increased resistance). The overstretched right atrium and right ventricle may also predispose to re-entry.

# A "VENOUS GREGG EFFECT" OF THE CORONARY CIRCULATION

Kim D. Chen, John K. Schofield, Konrad W. Scheel, Carl E. Jones, and Sue E. Williams.,
Department of Physiology, Texas College of Osteopathic Medicine, Fort Worth, TX 76107.

These experiments were designed to test the hypothesis that venous congestion produced by elevated right atrial pressure (RAP) causes a Gregg effect similar to that observed with elevated arterial pressure. In a blood perfused, beating, isolated dog heart preparation a saline filled balloon was attached to a vertical tube and inserted into the left ventricle. Oxygen difference was sampled from coronary inflow and the coronary sinus. Left ventricular end diastolic pressure (P-mmHg) and volume (V-ml), oxygen consumption, (MVO2 -ml/min), and total average left coronary flow (CF-ml/min) were recorded during maximum vasodilation. Compliance was calculated during late diastole as dV/dP. Another tube was inserted into the right atrium. RAP was increased from 0 (control) to 20 mmHg.

| Control | RAP | CF | MVO2 | dV/dP |
|---|---|---|---|---|
| Avg±SEM | 3.3±0.8 | 496±64 | 6.4±1 | 1.6±0.4 |
| | | % change | | |
| Avg±SEM | 11.5±0.6 | -7.7±1.5 | 24.2±9.8 | -13.6±3.4 |
| Avg±SEM | 21.0±1.0 | -16.9±3 | 45.7±24 | -31.0±0.5 |

We conclude that elevated RAP results in a "Venous Gregg Effect", reduces CF, and decreases left ventricular compliance.

**Clinical Relevance of increased right atrial pressures:**

We found that when right atrial pressure increases to pathological levels, as in heart failure, arrhythmias are precipitated, myocardial oxygen consumption increases, diastolic dysfunction occurs with a reduced efficiency of pump function. Decreased pump function is primarily due to coronary venous engorgement and decreased compliance of the left ventricle during elevated right atrial pressure.

(Supported by: Am. Heart Assoc., Texas Affiliate and NIH grant HL 35030).

**EVIDENCE OF ENDOCYTOSIS IN TOAD URINARY BLADDERS AS REVEALED BY SEM.** A.J. Mia, L.X. Oakford[1], H.F. Yancy, A.D. Davidson and T.Yorio[1]. Jarvis Christian College, Hawkins, TX 75765 and [1]Texas College of Osteopathic Medicine, Fort Worth, TX 75107.

Vasopressin (AVP) through $V_2$ and $V_1$ receptors enhances transmembrane water flow. AVP induces a shift in apical membrane microridges to microvilli, concurrent with activation of protein Kinase A, protein Kinase C and water channel insertion. The water channel is then internalized by endocytosis following removal of hormone. A time-course study was carried out using the techniques of scanning electron microscopy to correlate the events of apical membrane insertion and retrieval following withdrawal of hormonal actions. Urinary bladder sacs were set up with an imposed osmotic gradient and experimental tissues received 100mU/mL AVP for 10 min. Following withdrawal of AVP, tissues were allowed to incubate for 5, 10 and 20 min without the hormone. These tissues were fixed, postfixed, dried and mounted for viewing in the SEM. Control tissues, during pre- and post-rinse periods, showed normal phase of microridges in contrast to the expression of numerous microvilli in AVP-challenged tissues. At 5 min post AVP removal, endocytosis was evidenced in the form of invaginations at the apical membrane surface, which became prominent during the course of restoration of microridges by progressive endocytosis. At 10 and 20 min retrieval periods, many of these invaginations were further internalized to form endosome buds which eventually release into the cytosol. During the restoration process, some membrane invaginations showed lack of both microvilli and microridges which may represent membrane transitions during endocytosis following removal of hormonal actions.

Supported by US Army grants DAMD17-19-C1096 and DAAL03-92-G-0075.

# Clinical

# Abstracts 64 - 74

**PROTECTION OF LIPOPROTEINS AGAINST OXIDATION BY *CAPTOPRIL*.** L. Armstrong, Michael B. Clearfield, Stephen Weis, B.J. Kudchodkar and A.G. Lacko. Department of Medicine and Biochemistry and Molecular Biology, Texas College of Osteopathic Medicine Ft. Worth TX. 76107

This study was designed to determine the potential beneficial effects of the drug *Captopril* in the prevention the of the oxidation of low density lipoproteins (LDL) by evaluating lipid peroxide levels in LDL following oxidation *in vitro*. Lipoproteins were isolated by ultracentrifugation from fasing plasma to yield VLDL, LDL, HDL. Determination of lipid peroxides in LDL was carried out by the $CuCl_2$ oxidation method in the presence and absence of varying amounts of *Captopril*. The extent of LDL oxidation was also determined by monitoring the production of malondialdehyde.

The extent of oxidation and the degree of protection by Captopril were more pronounced with 10μM compared to 5 μM $CuCl_2$. *Captopril* was most effective protecting LDL compared to protecting HDL and VLDL against oxidation *in vitro*. Because the level of *Captopril* in the reaction mix (100 μg/ml) was considerably higher than the expected circulating level of the drug (~ 1 μg/ml), the dose dependence of its protective effect was investigated. The protection by *Captopril* was apparent even at low levels (20 mg/mL) and increased linearly with the dosage of the drug. *Captopril* also protected LDL against oxidation by lipoxygenase *in vitro*. At the level of 50 μg/ml, the protection (73% of control) was about the same against oxidation by lipoxygenase as it was against oxidation by copper (72%). Although the effect of *Captopril* in preventing the oxidation *in vitro* is impressive, it is difficult to determine what its impact might be *in vivo*. Further studies with patients are needed to assess the protective effect of *Captopril* against the oxidation of LDL by circulating oxidizing agents and enzymes (lipoxygenase) that undoubtedly accelerate the process of atherosclerosis and increase the risk of coronary heart disease.

# AUTOANTIBODIES TO PHOSPHOLIPIDS.

Z. Chen and W.J. McConathy, Department of Medicine, Texas College of Osteopathic Medicine, Fort Worth, Texas 76107

Anti-phospholipid antibodies (aPL) bind cardiolipin, phosphatidyl serine (PS), and a variety of other phospholipids. Studies were initiated to determine if autoantibodies to phospholipids may alter the metabolism of plasma lipoproteins. In developing our microELISA for autoantibodies, we initially examined a bank of 41 plasma samples. Of these, 20 % (n = 8) were positive for IgG autoantibodies to PS. A subset (25/40) of this bank were from hyperlipemic subjects (TC>240 mg/dl and/or TG>200 mg/dl) and 6 of the 26 were positive for aPL (23 % incidence). In contrast, only 2 of the remaining 15 (13 %) normolipemic subjects were aPL positive. In addition, we tested the sera from 160 normolipemic women of which only 4% were positive for aPL. This was consistent with literature reports of a frequency of 4 % in controls. We have also tested swine sera as a potential source of aPL to isolate autoantibodies for both in vitro and in vivo studies of lipoprotein and cellular surface binding properties. Of the 14 sera tested, 4 were strongly positive. These swine sera were also hypercholesterolemic (3 of 4, TC>300 mg/dl) and homozygote (4 of 4) for the ApoB genotype, *5/5*. Such observations suggest that in hyperlipemia, an increased incidence of autoantibodies to phospholipids may contribute to the inflammatory aspect of atherosclerosis disease processes and contribute to the incidence of atherosclerotic disease. It also suggests that with an increase in plasma lipids, an associated increase of immunoglobulins that bind phospholipids may occur. Whether this increase represents an immune response or an unrecognized function of IgG remains unclear. Such studies are relevant to heart disease, thrombosis, multiple sclerosis, and autoimmune diseases.

**ELECTRON MICROSCOPIC STUDY OF PORCINE AND CANINE SPINAL MENINGES.** M.T. Taylor, A.M. Brun-Zinkernagal, L.X. Oakford, and E.L. Orr. Department of Anatomy & Cell Biology, Texas College of Osteopathic Medicine, Fort Worth, TX 76107

The investing layers of the brain and spinal cord are an important but often overlooked aspect of the central nervous system (CNS). It is known that the meninges play major roles in maintaining the blood cerebrospinal fluid barrier, protecting of the CNS from injury and infection, and supplying conduits for the venous sinuses of the brain. However, many questions still remain regarding the structure and function of the meninges under normal and pathological conditions. This study describes our research on the structure/function of the meninges, with special emphasis on the arachnoid layer. Pig and dog spinal cords with meninges were carefully dissected out of the spinal canal after laminectomy and 3-5 mm cross sections were processed for electron microscopy. Meninges were evaluated by scanning (SEM; pig) and transmission (TEM; pig & dog) electron microscopy. TEM revealed that the fibrous dura was tightly packed with collagen and contained scattered fibroblasts. The electron dense dural border cells were flattened and contained scant cytoplasm. The arachnoid layer spanned five to ten cells thick. The interdigitating arachnoid cells were fairly electron lucent and contained numerous mitochondria and intermediate filaments. Junctional complexes and coated pits were also noted at the periphery of the cells. SEM revealed the presence of many fenestrae on the subarachnoid surface of the arachnoid while the dural side of the arachnoid exhibited no such spaces. There appeared to be collagen fibers and amorphous material in the intercellular spaces of the dural border cells and arachnoid. The subarachnoid space was spanned by arachnoid trabecular cells that surrounded and supported blood vessels and spinal rootlets. The pia consisted of one or two flattened cells overlying a large amount of connective tissue that harbored many blood vessels. (Supported by a Burroughs Wellcome Osteopathic Research Fellowship and a grant from the National Multiple Sclerosis Society.)

**CANINE AND PORCINE SPINAL ARACHNOID CELLS CULTURED ON PLASTIC AND MICROPOROUS MEMBRANES.** M.T. Taylor and E.L. Orr. Department of Anatomy & Cell Biology, Texas College of Osteopathic Medicine, Fort Worth, TX 76107

The arachnoid is located between the fibrous dura externally and the underlying subarachnoid space. Anatomical and physiological studies on the arachnoid suggest that it acts as a major component of the blood-cerebrospinal fluid barrier. This report describes initial studies of cultured arachnoid cells as an *in vitro* model of this barrier. Pig and dog spinal cords with their investing meninges were dissected from the spinal canal after laminectomy. The dura mater and denticulate ligaments were cut away and the arachnoid layer was carefully dissected away from the underlying subarachnoid adhesions. Under sterile conditions, the arachnoid was diced, tyrpsinized, centrifuged and placed in Minimum Essential Medium with fetal bovine serum, antibiotic-antimycotic, and L-glutamine. The cells were incubated at 37°C in 5% $CO_2$. The arachnoid cells, which have distinct nuclei and multiple nucleoli, started out bipolar then became polygonal. As the cells come into contact with each other, they formed parallel whorls and the cytoplasm was reduced. Primary cultures reached confluence in 10-14 days. For electrical resistance measurements, cells from passages 3-5 were seeded onto 6 $mm^2$ millicell-HA microporous membranes at a concentration of $2 \times 10^5$ cells/insert. Resistance was recorded across the cells and membrane for sixteen days, at which time cells were prepared for scanning and electron microscopy. Resistance rapidly increased from day one, plateaued at about day five and remained steady until termination of the experiment. The increased resistance is compatible with the establishment of numerous junctional complexes between arachnoid cells. (Supported by a Burroughs Wellcome Osteopathic Research Fellowship and a grant from the National Multiple Sclerosis Society. We thank A.M. Brun-Zinkernagal and Dr. L.X. Oakford for their technical assistance.)

**POLY(ADP-RIBOSE)POLYMERASE ACTIVITY - ASSOCIATION WITH RENAL INVOLVEMENT IN SLE.** R. M. Pertusi, H. Y. Chen, R. R. Rubin and E. L. Jacobson, Department of Medicine, Texas College of Osteopathic Medicine/University of North Texas, Fort Worth, TX 76107.

Systemic lupus erythematosus (SLE) is an autoimmune disease affecting multiple organ systems. Renal involvement occurs in about 50% of SLE patients. It is usually glomerular. Abnormalities seen on urinalysis include active sediment (cells and casts) and proteinuria. Progressive disease often results in reduced glomerular filtration rate. Poly(ADP-ribose) is synthesized from the niacin derived coenzyme, NAD, and functions in the repair of chromatin following DNA strand breaks. Among agents known to cause DNA strand breaks is ultraviolet light. Exposure to ultraviolet light is also known to cause exacerbation of SLE. Recently, an increase in the baseline number of DNA strand breaks was shown to be higher in SLE patients than in controls. Sibley et al. demonstrated decreased accumulation of ADP-ribose polymers in the peripheral blood lymphocytes of patients with SLE. We confirmed this observation, and through a variety of mechanistic studies determined that the decreased accumulation was a function of decreased poly (ADP-ribose) polymerase activity due to either altered enzyme function or decreased number of polymerase molecules. A review of the clinical characteristics of SLE patients in our study suggested that patients with renal involvement had lower poly (ADP-ribose) polymerase activities than those without renal involvement. Twenty-three patients fulfilling 4 or more American Rheumatism Association (1982) revised criteria for systemic lupus erythematosus (SLE) were recruited. Blood was drawn into unheparinized tubes, defibrinated, and spun on a ficol-hypaque gradient. The isolated mononuclear cells were subjected to hypotonic shock to permeabilize cell can nuclear membranes. Reaction buffer (containing DNAase) was added to initiate poly(ADP-ribose) polymerase activity. Radiolabeled NAD was incorporated into the forming polymers. The reaction was stopped using formic acid after ten minutes had elapsed. Counts were determined, and activity was expressed as pmols/10min/million cells. Systemic lupus erythematosus (SLE) patients wee considered to have renal involvement if they fulfilled criteria #7 of the American Rheumatism Association (1982) revised criteria for SLE which requires persistent proteinuria greater than 0.5 grams per day or greater than 3+ by urine dipstick if quantitation not performed OR cellular casts which may be red cell, hemoglobin, granular, tubular or mixed. Of the 23 SLE patients recruited, 7 were found to have renal involvement. Mean polymer accumulation for SLE patients with renal involvement was $126 \pm 94$. Mean accumulation for patients without renal involvement was $248 \pm 174$. A one-tailed independent t-test showed the two means to be significantly different ($0.025<p<0.05$). We conclude that lower poly (ADP-ribose) polymerase activities exists among SLE patients with renal involvement as compared to those without renal involvement. This study should be repeated using a larger sample size to confirm this observation.

INCIDENCE OF SOMATIC DYSFUNCTION IN THE GENERAL POPULATION. Sheila D. Page, D.O., J. L. Dickey, D.O., T. J. Wright, D.O., C. McKay-Hart, D. Fields, R. Erickson, J. Shores, Ph.D., and R. D. Page, D.O. Ph.D. Texas College of Osteopathic Medicine, Department of Manipulative Medicine, Fort Worth, Texas 76107.

An integral part of the prevention of disease and maintenance of health in Osteopathic medicine has involved the diagnosis and treatment of somatic dysfunction (SD). However, epidemiologic studies of SD in the normal population are not widely documented. The current study was initiated following the results of a pilot study (JAOA 90:9) designed to define the incidence of SD in the general population. Structural exams were performed on 196 persons to screen for SD. There were 137 females and 59 males with an average age of 39. The most prevelant disease states recorded by questionnaire were frequent low back pain (27%), migraines/frequent headaches (17.8%), urinary tract infections (17.3%), heartburn (12.7%), TMJ disease (10.2%), hypertension (9.6%), and arthritis (9%). The frequency distribution of SD was variable, ranging from 27% at T11 and 85% at OA. Discriminant analysis was used to build a model that described the various illnesses based on the findings of SD in this population. The predictability of hypertension was 100%, with SD at C4, T2, T4, T9, T12, and L4. A high predictability was also found in TMJ disease and migraines/frequent headaches with certain areas of SD. In conclusion, SD was found in all persons screened. A high frequency of SD was not found in all transitional areas of the spine as previously suggested by the pilot study. The data from the discriminant analyses suggest that SD is strongly associated with certain disease processes, however, further studies are required to determine the role of SD as a predictor of inherent diseases.

(Supported by AOA/Burroughs-Wellcome Fellowship F-91-07)

URBAN HEALTH PLANNING AND NEEDS ASSESSMENT IN AN AFRICAN-AMERICAN COMMUNITY: TWO APPROACHES. Sue G. Lurie, Ph.D., Department of Medical Humanities, Texas College of Osteopathic Medicine, Fort Worth, TX 76107/Department of Anthropology, University of North Texas, Denton, TX 76203.

Needs assessments for two urban health projects in an underserved community employed contrasting methods:
(1) Assessment of adolescents' health needs in Stop Six and Polytechnic planning districts was to compare responses of youth and adults on quantitative surveys (Lurie, Fabio, and Tabasuri). "Youth Survey" of 400 students using cluster samples of 100 each in two middle- and two high schools and "Adult Survey" of a random sample of 100 households included family, demographic, health and service data. "Youth Survey" results with school data were analyzed on SPSS (Higgins, UNT). Ethnicity was 81% African-American, 11% Hispanic, 2% Anglo, 1% Asian-American, 1% other. 64% reported preventive checkups but 44% did not get needed medical care. Most are usually healthy but report problems: overweight, 25%; headaches, 51%; stomach aches, 48%; depression, 37%; eating, 28%; pregnancy, 21%. 70 have long-term problems (asthma, 33). Health concerns for friends are: depression, 34%; marijuana use, 31%; venereal disease, 24%; physical and sexual abuse in family, 34%. Preliminary analysis of "Adult Survey" results indicate need for both adolescent and elderly health services. Study was non-funded. (2) Participatory assessment of "Health and Social Needs of Older Adults in Stop Six" for clinic planning used focus-group and qualitative interviews (Lurie) of 28 African-American elderly to complement a subsequent National Health Interview Survey (Eve, UNT) of a sample of 100. Qualitative analysis shows use of self-care for prevention, and common problems related to weight, diet, cholesterol, high blood pressure, heart, stroke, diabetes, vision, and hearing. Most have family support, need transportation and local clinic services. Study was funded by TIREA (TCOM/UNT). Design and implementation of assessments include variations in health planning and research roles of providers, academic researchers, and community planning groups.

PURSUING RELIABLE AND VALID MEASURES OF DIAGNOSTIC COMPETENCIES: AN ALTERNATIVE PERSPECTIVE

Papa FJ, Schumacker RE, Stone R, Young J.
Texas College of Osteopathic Medicine, GFP, Fort Worth, TX. 76107.

Standardized patient-based examinations have gained increasing acceptance as a means of assessing a variety of essential medical competencies. The authors however suggest that violations of accepted theoretical rationales preclude educators from using standardized patient-based examinations to draw valid inferences of an examinee's diagnostic competencies. The authors will subsequently describe the congruence between accepted rationales and those underlying a new artificial intelligence-derived diagnostic competencies assessment procedure. Following this description, the authors will report upon the reliability and validity of diagnostic competency measures derived from the new assessment procedure.
(Source of Support: (FIPSE) Fund for the Improvement of Post Secondary Education, and Smithkline Beecham AACOM/FOCUS).

DETECTION OF DEPRESSION IN THE FAMILY PRACTICE OFFICE USING A SELF-RATING SCALE

Vanderheiden, D., Shores, J., Hall, J., Kennedy, D.
Texas College of Osteopathic Medicine, GFP, Fort Worth, TX. 76107.

This is a study of the relative effectivesness of routine office visits, the Beck Depression Inventory and the Visual Analogue Rating Scale in the identification of depression in patients presenting to an ambulatory family practice clinic. Two hundred eighteen patients presenting for diagnosis and treatment voluntarily completed the Beck Depression Inventory and the Visual Analogue Rating Scale. When comparing Beck scores to recorded diagnosis(es), 90% of the depressed patients went undiagnosed. The Visual Analogue scale was found to be of value in identifying depressed patients. Use of the Visual Analogue scale increased the potentially depressed patient pool from 8 to 63. Use of the Visual Analogue scale also increased the occurrence rate of false positives from 1% to 20%. KEY WORDS: Outpatient, Family Practice, Diagnosis, Depression, Self-Report Scales. (Internal Support).

FACTORS INFLUENCING RETENTION OF MEDICAL OFFICE PERSONNEL by Robin Hall,D.O.

Texas College of Osteopathic Medicine, GFP, Fort Worth, TX. 76107.

The hiring retention of skilled office personnel in physician's offices is a recurring issure in office practice management. Factors that influence this process include salary, benefits, management style and perceived importance to the practice. This study varies from recent research that focuses primarily on physicians' opinions. The author identifies the opinions of medical and clerical staff as equally important and structured the data collection phase of this study for a more complete perspective. A description of the results of the survey that was mailed to all of the Osteopathic General and Family Practice physicians practicing in Tarrant County is included in this abstract. Five (5) questionnaires were mailed with return postage paid envelopes to one hundred and twelve (112) physicians' offices in Tarrant County. Employees that complete the questionnaires were asked to provide only age, sex and office position information, to insure anonymity and data accuracy. The survey includes medical practice and employee characteristics, employee benefits and job satisfaction data. The study suggests that a positive interpersonal work environment is a key in reducing employee turnover. No clear picture emerged regarding the importance of salary in this study.

(Internal Support).

# THE EFFECT OF TREATMENT OPTIONS ON PERCEIVED PAIN IN FIBROMYALGIA SYNDROME

Bernard R. Rubin, D.O., Cynthia Cortez, R.N., Gail Davis, R. N., Russell Gamber, D.O., and Jay Shores, PhD.. Texas College of Osteopathic Medicine, Department of Medicine, Fort Worth, Tx.

Fibromyalgia Syndrome (FS) is characterized by chronic musculoskeletal pain and palpable tenderness at specific anatomical sites. This study examined the effects of drug and manipulative therapy on the patients' perception of pain and each of five pain-related dimensions of quality of life. In this double blind study, 37 patients with FS were randomly assigned to one of four treatment groups. They received: 1) ibuprofen, alprazolam and manipulation, or 2) a placebo and manipulation, or 3) ibuprofen and alprazolam, or 4) a placebo drug alone. The treatment lasted 6 weeks. On first contact and at two week intervals thereafter, the subjects responded to a 5-item quality of life scale. A 15-item pain index was compared on their first and last visits. Multiple analysis of variance was used to test the effects of treatment over time. The treatment groups were found to be significantly different ($p \leq .05$) from on another. The use of manipulative therapy and a placebo drug resulted in significantly lower levels of perceived pain than did drugs alone, drugs with manipulation, or a placebo drug alone. These findings were reflective in 9 of the 24 pain-related ratings used in the study. The findings of this study confirm the effectiveness of manipulative therapy in the treatment of FS. The findings place in question the use of combined manipulation and drugs in the treatment of FS. The study suggest that drugs alone are slightly more effective in reducing perceived pain than a placebo alone.

# Eye

# Research

# Abstracts 75 - 92

**SLIME PRODUCTION IN OCULAR ISOLATES OF *STAPHYLOCOCCUS EPIDERMIDIS*.** Hoger, S.[1,2], E. Harris[2], A. Folkens[1], and B. Schlech[1]. [1]Alcon Laboratories, Inc., Ft Worth, TX 76134; [2]Texas College of Osteopathic Medicine, Ft Worth, TX 76107.

Extracellular slime composed of carbohydrates enhances some bacteria's ability to adhere to artificial or living surfaces. Slime production normally requires some source of available glucose as a carbon source in the growth medium. Glucose starvation turns off slime production in most strains of slime-producing coagulase-negative staphylococci. *Staphylococcus epidermidis* is a major ocular pathogen and we studied the level of slime production of 151 strains isolated from ocular infections. The Christensen tube method was used to detect slime production after growth in tryptic soy, nutrient, or modified sodium acetate media. In this study, about 30% of the strains produced some slime (17% heavy, 12% moderate, and 3% weak producers). Sixteen of these strains were studied further for their ability to produce slime under conditions of glucose starvation. We have shown that cultures deprived of glucose and other sugars for up to 19 days regain the ability to produce slime when grown for only one day in media containing sugar. A few strains, however, can produce slime when no sugars are present in the growth medium.

# PYSIOLOGICAL MODEL OF THE HUMAN CORNEAL EPITHELIUM

T. REESE[1], S. D. DIMITRIJEVICH[1], T. YORIO[2] & R. W. GRACY[1].
[1]DEPT. OF BIOCHEMISTRY AND MOLECULAR BIOL.,[2] DEPT. OF PHARMACOLOGY. TCOM.

The connection between transepithelial transport and corneal injuries of great significance in evaluation of ophthalmic pharmaceuticals and consumer products. *In vitro* models are frequently confluent cell monolayers featuring tight intercellular junctions (e.g. MDC kidney cells, the toad kidney A6 cell line), as indicated by a high electrical resistance (2-4 KW). Pericellular penetration of the test material through the monolayers, suggests the possibility of eye irritation or injury. Human corneal epithelial cells (CEPI) cultured on artificial membranes (Anocell™, Cellagen™), as confluent monolayers lacked an appropriate electrical resistance, and presumably the tight junctions. In contrast, tight junctions are observed between the surface layer cell in a stratified corneal epithelium *in vivo*. Once differentiation begins in vitro the electrical resistance rises, suggesting that an ocular model must have a stratified epithelium. When human corneal stroma fibroblasts (SFbs), are inoculated into a collagenous matrix, they form a translucent "stroma equivalent"(CSE), which also displayed low electrical resistance. CEPI cells, when plated on to the CSE, and induced to differentiate, form a multilayer epithelium. Scanning and transmission electron microscopy confirmed the presence of the basal, wing and desquamating surface cells. The alter exhibited desmosomal regions and microvilli characteristic of the authentic tissue. The electrical properties of the model will be discussed.

Supported by Grants from NIH, and The Tex. Adv. Res. Prog.

**LENS PROTEIN GLYCATION AND MIXED DISULFIDE LEVELS IN CULTURED RAT LENS.** Jaime E. Dickerson,Jr., Marjorie F. Lou and R.W. Gracy. Alcon Laboratories, Inc., Fort Worth, TX 76134 and Dept. of Biochemistry and Molecular Biology, Texas College of Osteopathic Medicine/University of North Texas, Fort Worth, TX 76107

Lens proteins are long lived proteins with those in the center of the lens predating the birth of the individual. As a result, they are subject to a host of modifications and damage through a variety of mechanisms. Two of these, glycation and mixed disulfide formation have been proposed as primary events which could cause conformational changes potentiating further modifications. We have utilized an *ex vivo* lens culture system to evaluate the hypothesis that lenses cultured with a high sugar (30 mM xylose or fructose) media will form higher mixed disulfide levels than controls. Xylose levels in the cultured lens rise rapidly (23 mM at 4 hr.)approaching media levels. The level of glycation after one week of culture is between 3-5% of total lens protein over control values. Mixed disulfide levels increase nearly 2X following one week of culture but this increase is independent of the media sugar content. These data indicate that glycation is not a major factor in mixed disulfide formation for this system.

**A NEW MIXED DISULFIDE SPECIES IN AGED AND CATARACTOUS LENSES.** Jaime E. Dickerson,Jr., and Marjorie F. Lou. Alcon Laboratories, Inc., Fort Worth, TX 76134 and Dept. of Biochemistry and Molecular Biology, Texas College of Osteopathic Medicine/University of North Texas, Fort Worth, TX 76107

The process of ageing in the normal human eye lens is unique among tissues due to the absence of turnover in the structural proteins. These proteins accumulate a variety of modifications throughout their lifetime. Significantly, the cysteine residues are subject to disulfide formation with low molecular weight thiol compounds present in the lens. We have previously shown the accumulation of glutathione and cysteine mixed disulfides in the proteins of normal human lens as a function of age. In this report we have identified a third mixed disulfide species $\gamma$-glutamylcysteine ($\gamma$-EC), by comparison with standards which we produced through two distinct methods. This new mixed disulfide is only prominent in old lenses (>60 years) and cataractous lenses. In these situations its level may approach those of cysteine mixed disulfide. The appearance of $\gamma$-EC may signal that the lens is in trouble and on the path of cataractogenesis. This protein modification may be a result of changes in the GSH biosynthetic pathway within the lens.

INTERRELATIONSHIP OF SORBITOL (SOR) AND MYO-INOSITOL (MI) LEVELS IN CULTURED BOVINE LENS EPITHELIAL CELLS. Rustin E. Reeves and Patrick R. Cammarata Departments of Anatomy and Cell Biology and Biochemistry and Molecular Biology, Texas College of Osteopathic Medicine/North Texas Eye Research Institute, Fort Worth, Texas 76107.

Purpose. The nature of the association between SOR formation and accumulation and MI uptake was examined in cultured bovine lens epithelial cells (BLECs) maintained in physiological medium (PM, 116 mM NaCl, 5.5 mM glucose) and sodium hypertonic medium (SHM, 232 mM NaCl, 5.5 mM glucose) during 1-8 days of continuous exposure.

Methods. Intracellular SOR and MI levels were determined with protein-free lysates of cultured BLECs by anion exchange chromatography and pulsed electrochemical detection using a Dionex BioLC chromatographic system.

Results. Exposure of cultured BLECs to SHM resulted in an enhanced capacity to accumulate both SOR and MI throughout a 3 day exposure period. The accelerated formation and accumulation of SOR and enhanced uptake of MI remained significantly above that of the PM control over the course of 3 days of incubation. BLECs maintained in SHM in the absence of the aldose reductase inhibitor (ARI), sorbinil, for up 8 days, likewise, displayed a continuous SOR accumulation. BLECs treated with SHM without ARI exceeded 190 nmol/ mg protein on the 8th day and, as expected, no intracellular SOR was detected in BLECs maintained in SHM plus ARI. On the other hand, although MI continued to accumulate throughout the 8 day incubation in SHM without added ARI, the capacity to take up MI from the medium under this condition remained significantly below that of BLECs treated with SHM plus ARI throughout the 8 days of continuous exposure (41 nmol/mg protein in SHM without ARI vs. 74 nmol/mg protein in SHM plus ARI after 8 days).

Conclusions. These results suggest a correlation between the rapid rise in intracellular SOR content and a decrease in the level of the free intracellular MI pool in cultured BLECs. The precise mechanism of this interaction with respect to elevated intracellular SOR content may involve (1) inhibition of MI uptake and/or (2) promotion of the efflux of MI and remains to be determined.

Supported by National Health Public Service Award EY05570 (PRC).

OSMOTIC SHOCK REPRESENTS A NOVEL INTERPRETATION OF THE OSMOTIC STRESS THEORY P.R. Cammarata and H.-Q. Chen Department of Anatomy and Cell Biology, Texas College of Osteopathic Medicine/North Texas Eye Research Institute, Fort Worth, Texas 76107.

Purpose. Past support of the osmotic stress theory came from studies showing a decline in intracellular myo-inositol (MI) in rat lenses exposed to 30 mM galactose overnight. This depletion of the MI pool was prevented by either the co-administration of an aldose reductase inhibitor (ARI) or by increasing the hypertonicity of the galactose medium with sorbitol, which, presumably, offset the osmotic effect of galactitol accumulation within the lens (Kawaba et al. *Invest. Ophthalmol. Vis. Sci.* 27: 1522-1526, 1986). We re-examined this data utilizing cultured bovine lens epithelial cells (BLECs).

Methods and Results. MI uptake is markedly stimulated in cultured BLECs exposed to increased extracellular sodium osmotonicity for 20 hr. The enhanced uptake involve increase in the maximal velocity without significant change in $K_m$ of both the high- and low-affinity MI transporters as indicated by Lineweaver-Burk analysis. Moreover, elevating the extracellular osmotonicity by the addition of raffinose, mannitol or sorbitol, likewise, enhanced MI accumulation (under conditions which did not favor intracellular polyol synthesis). Acute exposure (3 hr) of cultured BLECs to a range of 10-40 mM galactose plus sorbinil (i.e., conditions which would not permit galactitol synthesis) confirmed that galactose neither inhibits the high- nor the low-affinity MI transporter. The uptake of $^3$H-MI was lowered after chronic (20 hr) preincubation of cultured BLECs in 40 mM galactose (Gal, 305 ± 2 mosm) as compared to control cells in physiological medium (i.e., conditions which would favor galactitol synthesis). The co-administration of 150 mM sorbitol to Gal (455 ± 3 mosm) significantly increased, but failed to completely normalize, the MI uptake. However, the combined administration of 150 mM sorbitol and the ARI, zopolrestat, to Gal significantly exceeded the MI uptake observed with physiological medium (307 ± 3 mosm).

Conclusions. These results are not consistent with balancing the intracellular osmotic effect of galactitol accumulation in the lens cells by extracellular hypertonicity but rather suggest that the increase in MI uptake is due to an increase in the number (or, possibly, a change in the transporter turnover rate) of high- and low-affinity, sodium-dependent MI transporters expressed as a result of the osmotic shock stemming from exposure to hypertonic medium.

CLONING OF A 630 bp cDNA PORTION FOR THE $Na^+$/MYO-INOSITOL COTRANSPORTER FROM CULTURED BOVINE LENS EPITHELIAL CELLS (BLECs) USING THE REVERSE TRANSCRIPTION-POLYMERASE CHAIN REACTION (RT-PCR).

Cheng Zhou,[1,2] Neerai Agarwal[1] and Patrick R. Cammarata[1,2] Departments of Anatomy and Cell Biology[1] and Biochemistry and Molecular Biology,[1,2] Texas College of Osteopathic Medicine/North Texas Eye Research Institute, Fort Worth, Texas 76107.

Purpose. Myo-[$^3$H]inositol ($^3$H-MI) accumulation in cultured bovine lens epithelial cells (BLECs) occurred by high- and low-affinity, $Na^+$-dependent transport sites (Cammarata et al., Invest Ophthalmol Vis Sci. 33: 3572-3580, 1992). This observation has led to the suggestion that more than one MI transporter might be functioning in cultured BLECs, or that a single MI transporter might display two affinity states, each exhibiting different physical characteristics, influenced by the MI concentration. In order to begin to distinguish between these possibilities and establish whether the two MI transporters are coded for by one gene or, if, two independent genes exist for the two MI transporters, we cloned a portion of the cDNA for a MI transporter in cultured BLECs.

Methods and Results. Sense and anti-sense primers were designed based on a known, conserved region from a MI transporter in Madin-Darby canine kidney (MDCK) cells (Moo Kwon et al. J Biol Chem 269: 6297-6301, 1992) and subsequently utilized for the PCR. The cDNA was synthesized by reverse transcription using total RNA isolated from cultured BLECs, as well as from MDCK cells (positive control) with oligo(dt) as template. The PCR of the cDNA from BLECs and MDCK cells gave a 630 bp product which was gel purified and subcloned in a TA Cloning vector system (Invitrogen, San Diego, CA) and subsequently transformed to E. coli. Several colonies were picked and examined for the 630 bp insert by agarose gel. Using the dideoxynucleotide method (Sequenase USB, New Haven, CT), the nucleic acid sequences of the 630 bp cDNA from both the 3′ and 5′ ends were deduced and compared to the published sequence of the MDCK $Na^+$/MI cotransporter cDNA.

Conclusions. There was 100% sequence homology between the published cDNA of the MI transporter from MDCK cells and the PCR amplified product for MDCK cells. Moreover, there was greater than 90% homology between the BLEC and MDCK cDNA sequences. Thus, we have successfully isolated a cDNA encoding for a $Na^+$/MI cotransporter from cultured bovine lens epithelial cells.

Supported by National Health Public Service Award EY05570 (PRC).

**PHARMACOLOGICAL CHARACTERIZATION OF ALPHA2- ADRENERGIC RECEPTORS IN THE RABBIT CILIARY BODY.** Ying. Jin, Annita. Verstappen and Thoma. Yorio. TCOM\University of North Texas, North Texas Eye Research Institute, Ft Worth, TX 76107

The agonist- and antagonist- binding properties of $\alpha_2$-adrenergic receptors in the rabbit ciliary body membrane preparation were studied. Binding of agonist ligand, p-[$^{125}$I]iodoclonidine ([$^{125}$I]PIC), was characterized by a single high affinity binding site (Kd = 1.92 ± 0.24 nM and Bmax = 627 ± 92 fmol/mg). Inclusion of Gpp(NH)p in the assay decreased the specific binding by 25% but did not alter the Kd. Inhibition of [$^{125}$I]PIC binding by yohimbine, idazoxan and amiloride was determined to differentiate between $\alpha_2$-adrenergic receptors and imidazoline preferring receptors (IPR). Yohimbine and idazoxan inhibited all of the [$^{125}$I]PIC binding and their inhibition curves were consistent with a single class of binding sites suggestting that the [$^{125}$I]PIC binding sites in the rabbit cilliary body were $\alpha_2$-adrenergic receptors but not IPR. Subtypes of $\alpha_2$-adrenergic receptors were further studied by competition for [$^{125}$I]PIC binding with subtype-selective compounds. [$^{125}$I]PIC binding sites showed the pharmacologic characteristics of the α-2A adrenergic subtype (oxymetazoline >chlorpromazine >>prazosin) and competition by oxymetazoline and chlorpromazine was best fit by a single class of binding sites, indicating that the binding sites detected by this agonist ligand were α-2A subtype. Binding of the antagonist ligand, [$^{3}$H]rauwolscine, in the rabbit cilliary body membrane preparation also showed linear Scatchard plots (Kd = 6.79 ± 1.5 nM and Bmax = 653 ± 52 fmol/mg). However, inclusion of Gpp(NH)p in the assay did not affect either Kd or Bmax of [$^{3}$H]rauwolscine binding. Competition for this antagonist ligand by $\alpha_2$-adrenergic receptor subtype-selective compounds was also studied and compared with the ligand, [$^{125}$I]PIC.

CALCIUM SIGNALING IN CULTURED HUMAN ANTERIOR SEGMENT EPITHELIAL CELLS. Annita Verstappen[1], Dan Dimitrijevich[2] and Thomas Yorio[1]. Dept. Pharmacology[1] and Dept. Biochem. and Molecular Biol.[2], TX Coll. of Osteop. Med./University of North Texas, Ft. Worth, TX 76107.

The anterior segment of the human eye is subjected to chronic challenges by inflammatory mediators. Several of these mediators produce their effects through calcium signaling. However, the mechanism whereby the epithelial cells in this segment adjust to a continued stimulus is not well understood. Cultured human epithelial cells derived from the cornea, conjunctiva and nonpigmented ciliary epithelium (NPCE) were examined as to the presence of receptor-mediated intracellular calcium mobilization ($Ca_i$) and desensitization. In particular, the effects of histamine, substance P, EGF and $PGF_{2\alpha}$ on $Ca_i$ were investigated using single cell video imaging analysis (Universal Imaging) and fura-2AM. The resting $Ca_i$ (in nM) for conjunctival cells was $100 \pm 13$ (n=5), corneal epithelial cells, $77 \pm 9$ (n=24) and for NPCE was $80 \pm 11$ (n=6). Substance P and EGF were without an effect on $Ca_i$ mobilization in the cornea and NPCE, whereas histamine and $PGF_{2\alpha}$ produced dose-dependent increases in $Ca_i$ in all three cell types. The $Ca_i$ increased to $581 \pm 104$ nM (n=24) in the cornea following 10 μM histamine. The increase in $Ca_i$ was maximal within 30 sec and returned to baseline values within one min. The histamine effect appeared to be mediated by an $H_1$ receptor as pyrilamine and not cimetidine blocked the histamine-induced increase in $Ca_i$. Subsequent additions of histamine produced an attenuated response, even with higher doses of histamine, suggesting a rapid desensitization. The desensitization was not due to a depletion of intracellular stores of calcium, as thapsigargin still induced $Ca^{++}$ release following desensitization with histamine. The mechanism for desensitization is not clear but may involve down regulation of the $H_1$ receptor. However, other mechanisms are being investigated.

Supported by Orion Farmos and Alcon Laboratories, Inc.

**CARBACHOL-INDUCED INTRACELLULAR CALCIUM MOBILIZATION IN HUMAN CILIARY MUSCLE CELL LINE.** Shun Matsumoto and Thomas Yorio. Department of Pharmacology, Texas College of Osteopathic Medicine/University of North Texas, Fort Worth, TX76107

Ciliary muscle plays an important role in accommodation and regulation of aqueous humor outflow in the eye. Muscle cell contraction is thought to be regulated by changes of intracellular calcium concentration ($[Ca^{2+}]_i$). In this study, receptor-mediated effects of carbachol on calcium mobilization in human ciliary muscle cell was investigated using single cell fluorescent video-imaging analysis and the fluorescent calcium probe, fura-2/AM.

Human ciliary muscle cells were cultured on glass coverslip in 6 well-plates in 4 ml of Dulbecco's modified Eagle's medium (DMEM) containing 10% foetal calf serum (FCS). The media was changed into same amount of DMEM without FCS 24 hours before calcium measurement. The ciliary muscle cells on coverslip were cultured in HEPES buffered media containing 5 μM fura-2/AM for 60 min. $[Ca^{2+}]_i$ was measured by single cell fluorescent video-imaging analysis.

The resting $[Ca^{2+}]_i$ was 84 ± 8.1 nM (mean ± SEM, n=11). The addition of carbachol into the media caused a rapid increase in $[Ca^{2+}]_i$ in a dose-dependent manner. This rapid increase of $[Ca^{2+}]_i$ was followed by oscillation and did not show desensitization after repeated addition of carbachol. The carbachol-induced $[Ca^{2+}]_i$ oscillation was not observed in the absence of extracellular $Ca^{2+}$. Extracellular $Ca^{2+}$ is considered to be responsible for carbachol-induced $[Ca^{2+}]_i$ oscillation.

**EPIDERMAL GROWTH FACTOR STIMULATES DNA SYNTHESIS AND PROTEIN PHOSPHORYLATION IN CULTURED MÜLLER CELLS.** Rouel S. Roque[1], Ruth B. Caldwell[2], and M. Ali Behzadian[2]. [1]Dept. of Anatomy & Cell Biology & North Texas Eye Research Institute, Texas College of Osteopathic Medicine, Fort Worth, TX 76107; and [2]Dept. of Cellular Biology & Anatomy, Medical College of Georgia, Augusta, GA 30912.

Cultured rat Müller cells have high levels of epidermal growth factor (EGF) receptors (Roque et al., ARVO 1993). To evaluate the biological activity of this peptide growth factor, we studied DNA synthesis and protein phosphorylation in EGF-treated Müller cells. Müller cells, prepared from normal rats were immunoreactive for glial cell markers cellullar retinaldehyde binding protein, carbonic anhydrase-C, and S-100 at all passages used in these experiments. To determine the mitogenic effects of EGF, confluent cultures of Müller cells or 3T3 fibroblasts, grown in DMEM with 1-10% FBS, were incubated with 1 μCi of $^{3}$H-thymidine following EGF treatment (1-100 ng/ml). DNA synthesis, as measured by $^{3}$H-thymidine incorporation into TCA insoluble material, was increased in both cell types following EGF treatment. However, the induction of DNA synthesis by EGF was higher in Müller cells as compared with control 3T3 cells, reflecting the elevated number of biologically active EGF receptors in Müller cells. To study the immediate biological effects of EGF, we studied protein phosphorylation using immunocytochemistry, gel electrophoresis, Western blotting, and a monoclonal antibody against phosphotyrosines (PTyr). Immunoreactive PTyr were distributed primarily at the cell periphery, at focal contact sites and areas of intercellular contact. Intense reaction was also observed along filamentous cytoplasmic structures resembling stress fibers. Increased PTyr labeling, especially of cytoskeletal filaments, was observed following EGF treatment. The increased PTyr labeling was confirmed by Western blot analyses showing increased reactivity of the ~170 kD receptor and other related phosphoproteins (pp) including pp 110 and pp 92. These studies show that EGF stimulates DNA synthesis and phosphorylation of Müller cell proteins. Since growth factors have been implicated in Müller cell changes following injury, the increased $^{3}$H-thymidine labeling and induction of protein phosphorylation in Müller cells support a role for EGF in Müller cell transformation and/or proliferation during retinal disease. (Supported by American Heart Association, GA Affiliate and NIH-EY04618).

LIMBAL MAST CELL INVOLVEMENT IN EXPERIMENTAL AUTOIMMUNE UVEITIS IN THE LEWIS RAT. Carol H. Lee, Laura Smith Lang*, and Edward L. Orr. Department of Anatomy and Cell Biology and North Texas Eye Research Institute, Texas College of Osteopathic Medicine and *Alcon Laboratories, Inc., Fort Worth, TX, 76107.

The largest number of mast cells in the eye proper is found in the limbus. In experimental autoimmune uveitis (EAU), choroidal mast cells have been reported to degranulate and decrease in number early in the disease, leading to the suggestion that, in EAU, mast cell products may increase the permeability of retinal blood vessels and facilitate the access of immune cells to S-antigen (SAG) sequestered in the retina. To study possible limbal mast cell involvement in EAU, we injected Lewis rats with SAG in complete Freund's adjuvant (CFA) or with CFA alone. Clinical disease, affecting both the anterior and posterior segments of the eye, occurred 10 days post injection (pi). Four rats/day were sacrificed on days 5, 7, 9, 11, and 13 pi and the numbers of mast cells in choroids and limbi of fixed eyes were determined. We found that the number of limbal mast cells decreased in EAU and that the decrease in numbers occured prior to changes in choroidal mast cell numbers. Compared to controls, limbal mast cell numbers increased significantly on day 7 pi ($p<0.001$). In EAU rats, limbal mast cell numbers then decreased relative to day 7 pi values as the disease progressed (day 9 pi, $p<0.05$; day 11 pi, $p<0.05$; day 13 pi, $p=0.0001$). Choroidal mast cell numbers were not reduced significantly until day 13 pi ($p<0.005$). In addition, the histamine content of the anterior segment of the eye, which includes the limbus, iris, ciliary body, cornea, and lens, fell significantly in EAU ($p<0.0005$) by day 13 pi. (The limbus is the only part of the anterior segment with mast cells.) This decrease was concomitant with the appearance of increased histamine in the retina (significant on day 11 pi, $p<0.05$); and choroid (significant on day 11 pi, $p<0.05$, and day 13 pi, $p<0.01$). These results suggest that limbal mast cell products may mediate some of the inflammatory events which occur in the anterior chamber of the eye in rats with EAU.

**IN VIVO AND IN VITRO EVIDENCE FOR AGE-RELATED DECLINE IN RETINAL PIGMENT EPITHELIAL CELL SUPPORT OF PHOTORECEPTOR CELL SURVIVAL.** Harold J. Sheedlo, Wei Fan, Ning Lin and James E. Turner. Department of Anatomy and Cell Biology/North Texas Eye Research Institute, Texas College of Osteopathic Medicine/University of North Texas, Fort Worth, TX 76107

Normal neonatal retinal pigment epithelial (RPE) cell-transplants and RPE-cell conditioned media (RPE-CM) support photoreceptor cell (PRC) survival in retinas of Royal College of Surgeons (RCS) dystrophic rats and in a retinal cell bioassay, respectively. In this study, we investigated the PRC survival effect of normal adult RPE cells in the transplant and in vitro paradigms. RPE cells were isolated from neonatal and 2-4 and 17 month-old normal Long Evans (LE) rats. These cells were either transplanted into the subretinal space of 22-26 day-old RCS rats as isolated or cultured and passaged for either transplantation or CM collection. When analyzed 5 weeks post-transplantation, retinas of RCS rats transplanted with RPE cells from 2-4 month-old LE rats showed a 50% reduction in PRC layer thickness, when compared to RCS retinas transplanted with neonatal RPE cells. In addition, the thickness of the PRC layer in RCS retinas transplanted with freshly isolated or third-passaged RPE cells from 17 month-old LE rats and examined 2 months later was not significantly greater than that seen in control nontreated or sham-injected retinas of age-matched RCS rats. In a 3 day rat retinal cell bioassay, the number of surviving neonatal PRCs, as shown by opsin immunocytochemistry, in cultures supplemented with CM of rat RPE cells from 2-4 and 17 month-old LE rats was reduced by 55% and 95%, respectively, when compared to cultures supplemented with CM of primary neonatal RPE-cell cultures. However, CM of third-passaged RPE cells from 17 month-old LE rats supported PRC survival at a level seen in retinal cell cultures supplemented with neonatal rat RPE-CM. In conclusion, we have shown that transplants of adult rat RPE cells, either freshly isolated or passaged, have a reduced capacity to support PRC survival in RCS retinas, when compared to neonatal RPE cells. In contrast, CM of third-passaged adult normal RPE cells supported PRC survival in culture significantly above that of primary adult RPE cells, actually, at a level similar to neonatal RPE-CM. Thus, increased passage of adult RPE cells stimulates an upregulation of a factor(s) which positively affects in vitro PRC survival.

This work was supported by NIH grant EY 04337.

**THE EFFECTS OF ELEVATED GLUCOSE CONCENTRATIONS ON BOVINE RETINAL PIGMENT EPITHELIAL CELLS.** **Julie Y. Crider* **, Brenda W. Griffin*, and Thomas Yorio**. *Alcon Laboratories Inc., 6201 South Freeway, Fort Worth, Texas 76134, **Department of Pharmacology, Texas College of Osteopathic Medicine/University of North Texas, Fort Worth, Texas 76107.**

The retinal pigment epithelial (RPE) cell layer plays a vital role in the transport of molecules between the choroidal blood supply and the retina. Under pathological conditions such as diabetes, this function may be compromised. Bovine RPE cells were harvested from fresh eyes and typically were grown in uncoated dishes containing DMEM (4.5 g/l glucose) with 10% serum.

Cells at passage 4 were used in experiments involving alteration of glucose levels and the effects on $Na^+/K^+$-ATPase activity. $^{86}Rb$ uptake studies were performed on cells exposed to altered glucose levels for 2 days. Under various conditions, the maximal inhibition of the RPE cells to $10^{-4}M$ ouabain ranged from 37% to 63%. Preliminary dose response data indicate that the cells become increasingly sensitive to ouabain inhibition upon exposure to higher glucose levels.

**ISOLATION AND CHARACTERIZATION OF RETINAL PIGMENT EPITHELIUM (RPE) SPECIFIC cDNAs.**

N. Agarwal, Katherine O'Rourke, Zheng Liu, and R. Agarwal. Department of Anatomy and Cell Biology, North Texas Eye Res. Institute at Texas College of Osteopathic Medicine, Fort Worth, TX 76107.

Retinal pigment epithelium (RPE) plays an important role in the survival of neural retina. Any defect in molecular organization of RPE may result in photoreceptor cell death and/or visual dysfunction. Hence, the isolation of RPE-specific cDNAs will provide valuable candidate genes for identifying mutations responsible for inherited eye diseases including retinal degenerative disorders. A directional cDNA library was constructed from human RPE cells in Charon BS (-) phage vector and enriched for specific clones by using an efficient biotin-based subtraction method (Swaroop et al., Nucleic Acids Research, 19, 1954, 1991). Northern and cDNA Southern analyses of about 20 random cDNA clones from the subtracted library identified several cDNAs that are specifically expressed in the retinal pigment epithelium. One of these, AA35, detects a transcript of 1.5kb, and maps to human chromosome 3 p24-25. The sequencing and further characterization of AA35 will be presented. The molecular analysis and chromosomal localization of AA35 and other cDNAs should be helpful in obtaining probes for linkage analysis in families with genetic defects involving RPE function.

Supported by a TCOM Institutional grant and Fight for Sight Foundation.

**A Lack of Diurnal Cycle of S-antigen in *rds* Mutant Mice Retina May be Deleterious to Photoreceptors.**

N. Agarwal, Department of Anatomy and Cell Biology, North Texas Eye Research Institute at Texas College of Osteopathic Medicine, Fort Worth, TX 76107.

Despite the important advances in the molecular analysis of retinal degenerations in rodents and humans, it is still not clear why photoreceptors die. The events leading to photoreceptor cell death in one form of hereditary retinal dystrophy, as in the case of *rds* mutation, the dystrophy might be a result of a series of events which are precipitated by the lack of outer segments. Reduced phototransduction or light responses in *rds* mutation might result in the loss of proper signals at synaptic terminals, leading to abnormal release of neurotransmitters and/or trophic factors by target cells or the photoreceptor cell itself. In an effort to explore mechanisms for photoreceptor cell death we have studied the expression of S-Ag (arrestin, 48K) in *rds* and BALB/c retinas. In contrast to the normal diurnal variation in S-Ag expression in normal retinas, we report that this protein is expressed at high levels at all times in the *rds* mutant retina. A lack of a diurnal cycle and continuously high expression of S-Ag in *rds* retina might be a reflection of metabolic derangements in these cells which are not an obvious consequence of the underlying molecular defect in the peripherin gene. Studies of the mechanism of cell death in this mutant mouse model retina now take on increased significance since analogous mutations of the peripherin gene have been recently detected in some cases of autosomal dominant retinitis pigmentosa in humans.

Supported by a TCOM BRSG grant.

REGULATION OF MULLER CELL SURVIVAL AND DIVISION BY RPE: *IN VITRO* STUDIES OF A RETINA WOUND RESPONSE David Jaynes and James Turner, Department of Anatomy and Cell Biology, North Texas Eye Research Institute, Texas College of Osteopathic Medicine/University of North Texas, Fort Worth, Texas 76107

Induced and pathologic conditions of the retina often result in scar formation as a result of Muller cell (MC) activation. Upon activation these cells migrate, proliferate and, undergo changes in intermediate filament expression and morphology. Nothing is known at the present time as to what constitutes the signal(s) to activate this retina wound response. Previous studies have shown that medium conditioned by RPE (RPE-CM) supports, in as yet to be determined manner, MC survival and division when co-cultured with photoreceptors (Gaur et al., 1991). This study was undertaken to determine if the RPE cell directly affects MC survival and division. We isolated and cultured a pure population of MCs (Hicks and Courtois, 1990) from one to two day Long Evans rats at low density in the presence of RPE-CM or a defined medium (DM). First passaged MCs proliferated in the RPE-CM but failed to do so in the presence of only DM. Cells supplemented with RPE-CM began attaching to the substrate within one hour and, within one day, assumed a spread out morphology. These cells continued to proliferate for six days which was the longest time tested. In addition dying MC could be rescued by RPE-CM. This study offers strong *in vitro* evidence for direct RPE involvement in MC division. These findings also demonstrate the establishment of an *in vitro* model which mimicks a part of the retina wound response which can now be studied in greater detail.

**ACTIN FILAMENTS IN THE PHOTORECEPTOR CILIUM.** Michael H. Chaitin and Beth Burnside*, Dept. of Anatomy and Cell Biology and North Texas Eye Research Institute, Texas College of Osteopathic Medicine, Fort Worth, TX and * Dept. of Physiology-Anatomy, Univ. of California, Berkeley, CA.

The photoreceptor outer segment differentiates from the distal end of a 9+0 cilium and consists of a stack of membranous disks. New disks are continuously formed at the outer segment base from evaginations of the ciliary plasma membrane, while older disks are shed from the apex of the cell. Immunoferritin labeling has localized an actin-rich domain within the photoreceptor cilium, at the site where outer segment disk morphogenesis occurs. Binding of rhodamine-phalloidin has demonstrated that at least a portion of this actin is in the filamentous form. However, actin filaments have not previously been observed in electron micrographs of this region. In the current study, saponin-treated retinas from the rat and pinfish were incubated with myosin subfragment-1 in order to decorate the ciliary actin filaments with characteristic arrowhead complexes. After this treatment, a meshwork of decorated actin filaments could be detected within the center of the ciliary axoneme, at the base of the outer segment. Individual filaments radiated from the axoneme, and into the bottom of the outer segment disk stack, by passing between pairs of microtubule doublets. The arrowheads on these filaments uniformly pointed toward the cilium. The barbed (fast-growing) ends were associated with the plasma membrane and were oriented in the direction of disk expansion. These results suggest that an actin filament network may provide cytoskeletal support and guidance for the growing outer segment disks. (supported by NIH grant EY-06590 to Dr. Michael Chaitin)

# Substance Abuse

# Abstracts 93 - 100

THE EFFECTS OF ANXIOLYTIC AND ANXIOGENIC DRUGS ON THE SWITCH-OFF RESPONSE INDUCED BY AVERSIVE ELECTRICAL BRAIN STIMULATION OF THE PERIAQUEDUCTAL GREY. M. E. Jung, R. Depoortere, M. W. Emmett-Oglesby. Department of Pharmacology, TCOM, Fort Worth, TX 76107-2690.

Electrical brain stimulation (EBS) of the periaqueductal grey (PAG) has aversive/anxiogenic effects: a rat stimulated in this brain structure learns to press a lever to interrupt this stimulation (switch-off response). These experiments investigated the effects on the switch-off paradigm of an anxiogenic drug, pentylenetetrazole (PTZ), and of two anxiolytic drugs of the benzodiazepine receptor agonist class, diazepam (DZP) and abecarnil (ABC). A fourth drug, the benzodiazepine antagonist flumazenil (FLU), with no known anxiogenic or anxiolytic properties was also tested. Eight rats were first implanted bilaterally with 2 electrodes in the PAG; following recovery from surgery, they were trained to press a lever to interrupt EBS (train of pulses of 0.1 ms duration, frequency of 50 hz) applied to the PAG. After acquisition of stability of the switch-off response, they were tested at different frequencies (30, 40, 50 and 70 hz) following a 30 min pretreatment with vehicle (for control), PTZ (5, 10 and 20 mg/kg), DZP (1.25, 2.5 and 5 mg/kg), ABC (0.25, 0.5 and 1.0 mg/kg) or FLU (0.1, 1.0 and 10 mg/kg). Frequencies and doses for each drug were tested in a randomized order. The dependent variable was the switch-off latency (time elapsed between the onset of the EBS and its offset when the rat presses the lever). There was an inverse relationship between the frequency of the EBS and the switch-off latency. Higher frequencies produced shorter latencies to turn off the brain stimulation; this shorter latency is supposed to result from an increase in the aversiveness of the EBS resulting from the use of higher frequencies. PTZ, a drug known to cause anxiety in humans, significantly decreased latencies in a dose-dependent manner across all 3 frequencies tested (30, 50 and 70 hz). This decrease in the latency suggests that PTZ potentiated the aversiveness ot the EBS. Conversely, both DZP and ABC resulted in a significant and dose-dependent increase in the switch-off latency, suggesting this time that both drugs decreased the aversiveness of the EBS. FLU did not significantly modify switch-off latencies. These data demonstrate the ability of the switch-off paradigm to detect anxiolytic and anxiogenic as well as non-efficacious compounds in this switch-off paradigm. (Supported by NIDA grant RO1-3521.)

SELF-ADMINISTRATION OF COCAINE UNDER A PROGRESSIVE RATIO SCHEDULE IN THE RAT: TOLERANCE TO COCAINE. D.-H. Li, R. Depoortere, M. W. Emmett-Oglesby. Dept of Pharmacology, TCOM, Fort Worth, TX 76107-2690.

Sixteen Fisher 344 rats were first trained to self-administer cocaine (0.25 mg/100 ul) under a schedule where two presses on a lever produced cocaine injection. They were then trained under a progressive ratio (PR) schedule, in which an increasingly greater number of lever presses was required to be emitted for each subsequent cocaine infusion until the rats failed to emit the required number of presses within an hour. We termed the last cocaine injection as breakpoint, which indicated the total number of cocaine (reinforcers) the rats obtained. These rats were trained for over 50 daily sessions to assess the acquisition and stability of cocaine self-administration under the PR schedule. Subsequently,six rats were involved in a study of tolerance to the reinforcing effect of cocaine. They were given vehicle as a control or chronic cocaine treatment 20 mg/kg each time, three times a day for 7 days. The dose-effect curve for cocaine self-administration was tested before and immediately after termination of chronic treatment. The breakpoint showed a significant decrease across the entire dose-effect curve after chronic cocaine treatment compared to that of vehicle. Thus, in an animal model of drug liking, these data show that tolerance develops to the effects of cocaine.

INTRAVENOUS SELF-ADMINISTRATION OF COCAINE IN RATS: TOLERANCE AND CROSS-TOLERANCE. R.L. Peltier and M.W. Emmett-Oglesby. Department of Pharmacology, T.C.O.M., 3500 Camp Bowie Blvd., Fort Worth, Tx, 76107.

This experiment determined whether the chronic administration of cocaine would result in tolerance to cocaine, and whether the chronic administration of *d*-amphetamine would result in cross-tolerance to cocaine in a self-administration paradigm. Rats were implanted with indwelling jugular catheters and were allowed to self-administer cocaine (0.25 mg/injection) on an FR2 schedule of reinforcement, 15 reinforcers each day until stable baseline responding was observed. A dose-response curve for cocaine self-administration was then obtained for each rat using a multi-dose procedure. This procedure employs an FR2 schedule with a maximum of 24 reinforcers. The reinforcers are divided into three blocks of eight with each block of reinforcers providing a different dose of cocaine (i.e. reinforcers 1-8=0.5 mg/inj, 9-16=0.25 mg/inj and 17-24=0.125 mg/inj). After dose-response data was obtained, one group of rats was then infused with cocaine (20 mg/kg, i.v.) three times per day for seven days. The other group of rats was injected with *d*-amphetamine (3.2 mg/kg, i.p.) three times per day for seven days. During this chronic regimen, the rats were not allowed to self-administer cocaine. Twenty-four hours after the last infusion of cocaine, or the last *d*-amphetamine injection, a cocaine dose-response curve was again obtained. For both groups of rats, this dose-response curve was shifted approximately two-fold to the right. Following seven days without testing or training, all rats spontaneously returned to baseline rates of cocaine self-administration. These data show that chronic treatment with cocaine produces tolerance to cocaine, and chronic treatment with d-amphetamine produces cross-tolerance to cocaine in a self-administration paradigm. Supported by NIDA RO1 4137.

**ATTENUATION OF ALCOHOL WITHDRAWAL SYNDROME IN MICE THROUGH INTERVENTION WITH HYPERBARIC OXYGEN THERAPY.** W.A Stutts, MJ Forster, JR Wilson, EF Harris, Departments of Pharmacology, PHPM/HBOT, and Microbiology/Immunology, Texas College of Osteopathic Medicine/UNT, Fort Worth TX 76107.

The serious and extensive problems of alcohol dependence in humans is well-documented. Due to inherent difficulties in controlled studies of chronic alcoholics, a mouse model of ethanol withdrawal was developed in order to study the effects of hyperbaric oxygen therapy (HBO) on the withdrawal syndrome. In a relevant clinical study, patients in withdrawal from chronic alcoholism were treated with HBO at 1.3 to 2.0 atmospheres absolute (ATA) twice a day for one to three days. Fifty percent of patients had significant decreases in physiological and psychological symptoms without the aid of additional medication (Epifanova, 1988) In the present study a mouse strain (C57BL/6), known for ethanol tolerance, was fed a nutritionally complete liquid diet which contained 37% ethanol (water ad libitum). A control group was fed an isocaloric liquid diet with the ethanol calories replaced by sucrose. Liquid diet consumption and weights were monitored daily for seven or nine days. On withdrawal days (Day 8 or 10, respectively) all liquid diets were replaced with laboratory food and half of the ethanol-fed mice were randomly selected for HBO treatment while the other half received no treatment. Treatment consisted of two 60 min sessions at 1.5 ATA spaced eight hours apart. Withdrawal signs were monitored in all groups for 12 hours at two hour intervals using a standard rating scale. The survival of the 7-day , ethanol fed, HBO treated group was 90% but only 56% in the 7-day, ethanol fed, non-treated group. The survival of the 9-day, ethanol-fed, HBO-treated groups was 60% but only 20% in the 9-day ethanol-fed, non-treated group. Total withdrawal scores after 7 days for the HBO-treated mice were 21.2 ± 2.2 (mean ± SEM) as compared to non treated (29.8 ± 2.9). Total withdrawal scores after 9 days of ethanol diet were 23.7 ± 3.5 for the HBO treated mice as compared to 31.6 ± 2.6 for the non-treated mice. The 9 day feeding resulted in a withdrawal period longer in duration and more severe in intensity, as evidenced by higher scores indicating more profound symptoms. These preliminary results indicate some potential for HBO in the effective management of ethanol withdrawal. If so, HBO would be clinically useful due to its minimal potential for addiction when compared with pharmacological interventions.

**Potential Role of $5HT_{1C}$ and/or $5HT_2$ Receptor in the Mianserin- induced Prevention of Anxiogenic Behaviors Occurring During Ethanol Withdrawal**

Rezazadeh, S.M., Wallis, C.J., and Lal, H. Department of Pharmacology, Texas College of Osteopathic Medicine, Fort Worth, Texas, 76107.

Drugs which selectively decrease serotonergic (5HT) neurotransmission, reduce anxiogenic behaviors in a variety of animal models. This study was conducted to determine whether a single dose of mianserin, administered 48h or 7d prior to testing, could prevent the anxiogenic behaviors observed during ethanol withdrawal. Rats were fed a liquid diet containing 4.5% ethanol for 4d. They were tested 12h (acute withdrawal) and 5d (protracted withdrawal) after the last ethanol dose. Both the % of time spent on, and the % of entries made onto the open arms of an Elevated Plus Maze (EPM) were significantly reduced during withdrawal. Such performance normally parallels behaviors elicited in anxiogenic environments. Mianserin (2.5-20 mg/kg, ip), injected in a single dose on the morning of the 3rd day of ethanol administration, i.e., 48h and 7d prior to testing, dose dependently prevented the effect of ethanol withdrawal. Further, the $5HT_{1C}$/$5HT_2$ receptor agonist (+/-)-1-(2,5- dimethoxy-4-iodophenyl)-2-aminopropane HCl (DOI) did not affect behaviors in the EPM in ethanol-naive rats, nor in those undergoing ethanol withdrawal. However, inspite of a marked tolerance to DOI- induced body shakes (a measure of $5HT_2$ function) during withdrawal, DOI reversed the preventative effect of mianserin in the EPM. In contrast, 1-naphthyl-piperazine (1-NP) reduced open arm activity in ethanol-naive rats, and this action was enhanced during withdrawal. In addition, the effect of mianserin pretreatment was reversed by 1-NP and this pretreatment also produced a shift to the right in the dose-effect curve of 1-NP during ethanol withdrawal. Unlike the pure agonist DOI, 1-NP has agonist properties at $5HT_1$ but antagonist properties at $5HT_2$ receptors. Thus, mianserin exhibited long term efficacy in preventing a symptom of ethanol withdrawal which may be related to down regulation of a specific $5HT_1$ receptor subtype, possibly the $5HT_{1C}$, but not the $5HT_2$ receptor. Supported by NIAAA Grants AA06890 and AA09567.

EFFECT OF ETHANOL ON ADENOSINE RECEPTORS CONTRIBUTES TO THE DEVELOPMENT OF THE WITHDRAWAL SYNDROME.

C.J. Wallis, S.M. Rezazadeh, and H. Lal Department of Pharmacology, Texas College of Osteopathic Medicine, Fort Worth, TX, 76107.

It has been hypothesized that stimulation of adenosine receptors is involved in ethanol (ETOH) intoxication and the development of tolerance. We investigated an ethanol withdrawal symptom ("anxiety-like" behaviors) using the elevated plus maze (EPM) paradigm (Lal et al., Alcohol 8:467, 1991). Long-Evans hooded rats were given a balanced liquid diet containing 4.5% ETOH for 10 d (Lal et al., JPET 247:508, 1988). Twelve h after a final ETOH dose (3g/Kg, po), rats were tested in the EPM. We observed a significant reduction in the open-arm activity and the number of total arm entries indicative of ETOH withdrawal. Pre-treatment with an A1 adenosine agonist, R(-)-N6-(2-phenylisopropyl)-adenosine (PIA, 0.08-0.32 mg/Kg, ip, 15 min), had little effect on performance in the EPM during ethanol withdrawal. Acute treatment with an A1 adenosine antagonist, 8-cyclopentyl-1,3-dimethylxanthine (CPT, 0.02-0.16 mg/Kg, ip, 60 min), exacerbated ETOH withdrawal with a further reduction in open-arm activity. Chronic treatment with CPT ( 0.04-0.16 mg/Kg, ip, 2X/d) during the last 6 days of ETOH diet administration resulted in a dose related increase in the amount of time spent in the open-arms of the EPM, but had little effect on the number of total arm entries. These data support the hypothesis that an ethanol stimulated increase in adenosine receptor activity may be associated with the development of dependence and that blockade of adenosine receptors during ethanol treatment reduces the display of "anxiety-like" behaviors during ethanol withdrawal. Supported by NIAAA Grants AA06890 and AA09567.

# MURINE MODEL OF ETHANOL-INDUCED IMMUNOMODULATION DURING STRESS INDUCED CONDITIONAL BEHAVIORAL DESPAIR.

William A. Stutts, Judy Wilson, Elizabeth F. Harris, and Peggy Gracy, Departments of PHPM/HBOT and Department of Microbiology/Immunology, Texas College of Osteopathic Medicine/University of North Texas, Fort Worth TX 76107 and University of Texas Southwestern Medical Center, Dallas, TX 75225.

Alcohol abuse has been associated with an increased susceptibility to infectious diseases and certain tumors. On the basis of these observations an effect of ethanol on the immune system has been suggested. Various types of stressors have been shown to alter the parameters of immunocompetency in animals and humans as well. To investigate the relationship of these two variables we have used a mouse model system in which male C57BL/6 mice were administered ethanol (20% w/v) in drinking water. Consumption averaged 8.5± 0.5g/Kg per animal/day. To assess the role of stress, a model of conditional behavioral despair (forced swim) was used. Groups of mice were subjected to daily six minute swimming trials. In this model, after initial vigorous activity, the animals become conditioned to immobility and stop swimming (learned helplessness). Groups included alcohol consuming and stressed mice, alcohol only, stress only, and caged controls. The effects were determined on natural killer (NK) cell lysis and the mitogenic response of splenic lympocytes to ConA and PHA. Alcohol showed increased NK cell lysis at all time periods; stress lowered NK cell lysis of 2 wks. with high recovery at 3 wks. Alcohol and stress severely depressed lysis after 1 wk; but recovered after 2 wks. Lymphocyte mitogen responses of alcohol only groups were increased at wks 1 and 2 but severely depressed after 3 wks. Stress only decreased mitogen responses after 2 wks. Stress and alcohol groups showed increased mitogen activity at all time periods when compared with alcohol or stress only groups suggesting a possible protective mechanism of one stimulus on the deleterious effects of the other on the immune response. An age difference appears to exist between young and old mice with the young mouse lymphocytes being more sensitive to the effects of ethanol at all time periods.

100

**COMPARISON OF THE EFFECT OF VARIOUS ALDOSE REDUCTASE INHIBITORS ON NAPHTHALENE CATARACT IN RATS.**

Gou-Tong Xu, Marjorie F. Lou and J. Samuel Zigler*. Alcon Lab., Inc., Fort Worth, TX 76134. *NEI,NIH,Bethesda, MD 20892.

The cataract caused by naphthalene in experimental animals is thought to be a good model for human age-related cataract. Our previous study showed that cataracts can be induced in vivo by feeding rats with naphthalene(1.0 g/kg/day) and in vitro by exposing rat lens to naphthalene dihydrodiol (2.5 X $10^{-5}$M) and also AL01576 (an Aldose Reductase Inhibitor) can completely prevent such a cataract both in vivo and in vitro. To further understand the action site of AL01576,we compared the effects of various classes of ARIs including AL01576, AL04114, Sorbinil and Tolrestat on rat naphthalene cataract as well as a dual cataract model induced with galactose and naphthalene. At the same dosage (10mg/kg/day), both AL01576 and AL04114 completely prevented all morphological and biochemical changes in the lenses of naphthalene-fed rats. However, Sorbinil showeded a much weaker efficacy in this model and Tolrestat showed no efficacy at all. In the dual cataract model, Tolrestat prevented galactose cataract formation and reduced the lens dulcitol accumulation, but showed no protection against the shell-like opacity caused by naphthalene, whereas AL01576 can protect the lens from both stresses. AL04114, a dimethoxy derivative of AL01576 and a noninhibitor to cytochrome P-450, demonstrated similar efficacy as AL01576 in preventing naphthalene cataract formation. All these results indicate that the drug action of AL01576 or AL04114 in naphthalene cataract inhibition may be targeted at dehydrogenase or related enzymes involved in the naphthalene dihydrodiol metabolism. The inhibition of aldose reductase or cytochrome P-450 may not be involved in the prevention of such a cataract.

# Nutrition

# Abstracts 101 - 102

ASSESSMENT OF NIACIN STATUS IN AN ELDERLY POPULATION. J. A. Knebl & E. Jacobson. Department of Medicine, Texas College of Osteopathic Medicine, Ft. Worth, TX 76107.

Nutritional deficiencies exist in an older population related to a comination of social, economic, physiological, psychological and adverse health conditions. Data on niacin nutrition in the elderly is very scanty, due in part to the lack of a good biochemical method of evaluation.

A new method to assess niacin status has been developed by this laboratory. This method measures erythrocyte NAD and NADP content, which has been shown to reflect dietary niacin intake (Fu, et.al., J.Nutri. 119:1949-1955, 1989). The data are express as niacin number which is equal to [NAD/(NAD + NADP)] X 100%. Normal values for young adults have been established at 57 to 69.

Data abtained on 77 geriatric outpatients revealed a wide reange of niacin values with 22% below the normal range for young adults. Conversely, 3% had greater than normal values and all were taking niacin supplementation. Assessment of niacin status by this newly developed assay may determine those geriatric patients at risk and predict the need for intervention.

ESTIMATING CALORIC REQUIREMENTS IN AN ELDERLY POPULATION. J. Knebl, D. Ostransky, & R. Osborn. Department of Medicine, Texas College of Osteopathic Medicine, Fort Worth, TX 76107.

The accurate prediction of caloric requirements in the elderly is important for determining nutritional status and needs. With aging there is a decrease in resting energy expenditure (REE) parallel to a decline in body mass. The clinical estimate of REE has traditionally been derived from a prediction equation developed by Harris and Benedict (HB) in 1919. The HB equation predicts basal energy expenditure (BEE) which is multiplied by a factor of $\geq$ 1.2 to approximate REE. The study included 239 subjects, only 38 were over the age of 65. Our purpose was to validate the usefulness of the HB method for REE for an elderly population. Nineteen subjects aged 65 - 85 (x=73) underwent a history and physical examination, complete nutritional assessment and REE by indirect calorimetry (Medical Graphics CAD 200, St. Paul, MN). The measured REE was compared to the calculated BEE. There a significant correlation between the measured REE (1345.63 $\pm$ 299.33 kcal), with $r = 0.71$, $p \leq .001$. This study suggest that the calculated REE based on the HB equation overestimates REE in an elderly population.